IMPERIAL COLLEGE LONDON

Department of Earth Science and Engineering

Centre for Petroleum Studies

Foam EOR Processes

By

Olivier Howaizi

A report submitted in partial fulfilment of the requirements for the MSc and/or the DIC.

September 2014

DECLARATION OF OWN WORK

I declare that this thesis

Foam EOR processes

is entirely my own work and that where any material could be construed as the work of others, it is fully cited and referenced, and/or with appropriate acknowledgement given.

Signature:.....

Name of student: Olivier Howaizi

Name of supervisor: Professor Sam Krevor

Name of the company supervisor: Marie-Ann Giddins, Daniel Dias, Konstantinos Makromallis

Acknowledgements

First, I would like to warmly thank my supervisors, Marie Ann Giddins (Schlumberger) and Doctor Samuel Krevor (Imperial College) for having proposed me this project, and providing me with precious help all along these last 3 months.

Then, my thoughts go to my mentors from Schlumberger, Daniel Dias and Konstantinos Makromallis, for their patience and their availability.

Finally, I would like to thank the other interns from Schlumberger, Sam Cotteril, Bhavik Patel, Mansour Khelifa, Rafay Zafar, Mohsin Naveed and Louis Cleret de Langavant for the long conversations and precious solidarity through this project.

Table of Contents

List of Figures

List of Tables

MSc in Petroleum Engineering 2011-2012

Imperial College London

Foam EOR Processes

Olivier Howaizi

Professor Sam Krevor, Imperial College London

Marie Ann Giddins, Daniel Dias, Konstantinos Makromallis, Schlumberger

Abstract

After the success of the foam injection in the Western Fault Block of the Snorre Field in in the late 90's, the FAWAG (Foam Assisted WAG) process is considered to have good potential for enhanced oil recovery. Foam has the ability to delay the gas breakthrough, thanks to a better gas mobility control, fluid diversion, and gas blocking, which results in a better recovery.

The main objectives of this paper have been to build an empirical model and a chemical reaction model with two commercial simulators, a blackoil simulator and a compositional simulator. Sensitivities have been run on both of them to measure the impact of variations in key parameters and evaluate which simulator best depicts reality. A comparison of the mechanistic characteristics between the two models has been done, in order to provide a characterization of foam behaviour. Specific attention has been focused on the adsorption and decay phenomena, which are often underrated. In the compositional simulator, adsorption and decay are represented by chemical reactions. In the black oil simulator, empirical formulae are used.

The models have been based on information about the Snorre Field, but are more simplistic to better capture the influence of each foam parameter. The models that have been built comprise 192 000 cells and 5 layers of different porosity and permeability, with one vertical gas injector, one vertical water injector, and one vertical producer well. In a 4000 days long simulation, one SAG (Surfactant Alternating Gas) cycle has been performed, including one slug of surfactant solution and one slug of gas, with a ratio of 1:3.

The SAG process simulation appears to be very sensitive to the grid size, especially in the vertical direction. This could imply real problems in full field models, considering the fact that foam models include non-linear equation, leading to time consuming simulations.

The biggest impact on the recovery factor is caused by the foam concentration and the reference mobility reduction M_r which can cause a significant breakthrough delay difference. However, if the foam is too effective, then the mobility of the injected fluid is too low; injection pressure will be too high and there will be no positive improvement in production.

In this study, the production profiles are comparable in both models when the foam is not too effective. It is possible to calibrate the decay process, if the chemical reaction transforming foam into water has a reaction order of 1. For the adsorption process, a calibration is mathematically possible, but only if the adsorption reaction is treated as instantaneous. For this reason, there are advantages in using the compositional simulator when dealing with foam.

Introduction

Foam has been widely used for EOR processes since the Snorre field Pilot, first described by Svorstol et al. (1996). Skauge (2002) and Aarra (2002) estimate that the expenses for FAWAG (Foam Assisted WAG) on Western Fault Block was 1M USD, and additional oil recovery value was around 30M USD. Foam injection is especially used when early gas breakthrough is expected during a WAG process. If the reservoir is heterogeneous, high permeability layers, called thief zones, are likely to create a bypass for the injected gas, which will increase the Gas Oil Ratio and decrease the recovery factor. Furthermore, during a WAG process, gas tends to rise up at the top of the surface due to the density differences with water and oil, which leads to early gas breakthrough as well. Foam can mitigate these problems, as it enables to improve the sweep efficiency, to reduce the gravity segregation, and smooth the heterogeneities. The modelling of its effect through porous media is very complex. Ma et al. (2014) have reviewed the different modelling techniques for foam, including gas reduction methods, population balanced methods, local equilibrium method, or gas viscosity alteration method.

The two simulators that we have used for this study have different characteristics. The first one is a black oil simulator, and considers foam and surfactant as tracers. It takes into account the adsorption on rock surface and decay over time. The use of foam in black oil simulation has been widely studied by Cheng (2000), Aarra(2002), Shan (2004), Spirov (2012) and Rossen (2013). Especially, a lot of attention has been drawn on the Snorre Field, only FAWAG public data available. The second simulator is a compositional one: chemical composition of oil and water are used and it includes chemical reactions. This is the first time the use of foam as a chemical component in this simulator has been studied. With two very different ways of depicting foam, some drastic differences should be expected between both simulators. The main goal of the study has been to

create an exhaustive comparison of the two simulators, to study the differences of behaviour and to determine which one should preferentially be used when dealing with foam injection strategies. In particular, this study has been focusing on the gas breakthrough delay caused by foam, one of the best indicators of foam efficiency.

To describe the effect of foam, such as viscous fingering reduction, gravity segregation diminution or gas breakthrough delay, both simulators use the model depicted by Blaker et al. (1999). Cheng and Rossen (2000) confirmed that it fitted foam behaviour at high and low quality regime reasonably well. In this model, we assume that foam has an impact on gas mobility, which is its ability to move through interconnected pore space. This mobility will be reduced by a reduction factor M_{rf}

$$M_{rf} = \frac{1}{1 + M_r . F_{sc} . F_w . F_o . F_c} \quad \text{..... (1)}$$

This reduction factor includes a function of surfactant concentration F_{sc}, which will measure the influence of the surfactant concentration on the model. The more concentrated the surfactant concentration is, the more effective the foam will be.

$$F_{sc} = \left(\frac{C_s}{C_s^r}\right)^{e_s} \quad \text{..... (2)}$$

The reduction factor also includes a function of water concentration F_w, which will measure the influence of the water concentration on the model. The presence of water is essential for the foam to be stable. If not enough water is present in the rock there is a foam dry out phenomenon that weakens the foam (Cheng 2000). This is depicted by F_w where

$$F_w = 0.5 + \frac{\tan^{-1}(f_w . (S_w - {S_w}^r))}{\pi} \quad \text{..... (3)}$$

Oil also has an influence on the stability of the foam, as it increases the degree of foam coalescence. Mannhardt (1998) estimates that oil becomes detrimental to foam if $S_o > 0.05 - 0.2$. In our model we define F_o as:

$$F_o = \left(\frac{S_o^r - S_o}{S_o^r}\right)^{e_o} \quad \text{..... (4)}$$

Finally, Nguyen (2000), and Cheng (2000) describe the foam as a shear thinning fluid. As a consequence of this, the capillary number has an influence on the gas mobility reduction, and so we define F_c in our model

$$F_c = \left(\frac{N_c^r}{N_c}\right)^{e_c} \quad \text{..... (5)}$$

Therefore, if the gas flows without foam in the reservoir is governed by Darcy's law

$$q_{g,\text{no foam}} = \lambda_g \overrightarrow{\text{grad}}\, P \quad \text{..... (6)}$$

Then, with foam,

$$q_{g,\text{foam}} = M_{rf} . \lambda_g . \overrightarrow{\text{grad}}\, P = M_{rf} . q_{g,\text{nofoam}} \quad \text{..... (7)}$$

The foam model of our simulator will also include the decay of foam and the adsorption of foam. Adsorption of rock comes from a physical or chemical interaction of foam with the surrounding rock. It results in an adhesion of one part of the foam molecules, making them inactive, so the foam effective concentration in the pores decreases. Decay is a cause of alteration of foam effectiveness, assuming that with time, activeness of the foam naturally decreases.

A.R. Awan (2006) and Spirov (2012) explained that the best overall WAG ratio for most North Sea fields is 1:1. However, particular cycles from simulation studies of FAWAG cycles, are detailed by Spirov (2012), or Aarra and Skauge (2002), and among them we find short cycles with WAG ratio of 1:2 or even 1:9.Shan (2004) explains that one large SAG (Surfactant Alternating Gas) cycle gives better sweep efficiency than numerous small SAG cycles. In our case, we will especially focus on the gas breakthrough. For this reason the gas slug will last longer than the water slug so we can observe the gas breakthrough soon enough. Only one SAG cycle will be performed to be sure to observe the gas breakthrough during the same cycle in each case. Aarra (2002) relates that the distance between the injector P32 and the producer P39, which were used in the Snorre Field for the first FAWAG strategy, was 1500m and gives some permeability data for the Upper Statfjord reservoir zones S1 and S2 of the Snorre field, affirming that in the best reservoir zones, the permeability is comprised between 400mD and 3500 mD. Our reservoir model will be slightly shorter, only 1500 feet long, with a 900 feet-distance between the two wells. More details on the model are available in *table 5* and *table 8.* Thanks to Spirov (2012), we know that the Foam Surfactant AOS has been mainly used in the Snorre Field. Brierly-Green and Gee (1999) give us a range of 190-220 g/mol for the molecular weight of AOS. Aarra (2002), gives the best parameters of Surfactant concentration function to achieve a good match for Snorre Foam cycles, with C_s^r =0.0000058 mol fraction (0.023 lbm/stb) and an exponent factor e_s of 1. The injected surfactant also goes from 70 to 174 lbm/stb of water. These foam parameters from the Snorre Field will enable us to have enough information to create our own artificial model, which will focus on the influence of the key parameters and their impact on the breakthrough delay.

Methodology and Analysis

Definition of oil properties

A compositional model can be defined, and the corresponding blackoil tables extracted to model the same oil in both cases. A first step in this study was to determine what kind of oil would be suitable for both simulators, and would give the same results for a given WAG (water alternating gas) and SAG (surfactant alternating gas) strategy. For this purpose, a simple 3D model was created and production strategies were performed on it. Before being validated, the main characteristics of production should match in both simulators, before creating a more complex model, including foam, WAG and SAG strategies. One of the main goals is to avoid the phase change or miscibility during depletion, water imbibition, or gas injection. Comparable behaviours for the two simulators during these simple strategies will allow us to build a comparable model for a more complex SAG strategy.

Test grid description	
Number of cells	1000
(DX, DY, DZ)	(10, 10, 10)
Pore Volume	891 000 rb
STOIIP	592 000 stb
GIIP	155 000 MSCF
WIIP	173 000 stb
Datum depth	9200 ft
Pressure at datum depth	970 psi

Table 1: Characteristics of the test grid used for the reservoir oil definition

Strategy	Strategy 1	Strategy 2	Strategy 3
Type of strategy	Depletion	Water injection	Gas injection
Time of simulation	1 year	4000 days	4000 days
Injection rate	None	350 stb of water per day	250 MScf of gas per day
Bottomhole injection pressure limit	None	1300 psia	
Oil production rate	300 stb/d		
Bottomohole production pressure limit	950 pisa		

Table 2: Different strategies tested on Test Grid to define the oil in place properties and the nature of the injection gas

The first objective is to check that the oil in the reservoir conditions has the same production characteristics for a simple depletion strategy. As seen in *fig.1* with the chosen reservoir fluid, the reservoir average pressure, oil production rate and gas production rate match between both simulators for a 1 year depletion strategy, with an oil production plateau of 300 stb per day and a gas breakthrough occurring after 2 months. The same check is done for a simple 10 years water injection strategy. As seen in *fig.2* with the chosen reservoir fluid, there is a good match for both simulators during the whole process, with a 300 stb/day oil production rate plateau of 2.5 years and a gas production plateau of 300 MScf/day. Almost every chosen reservoir fluids gave a good match for the depletion and water injection strategy.

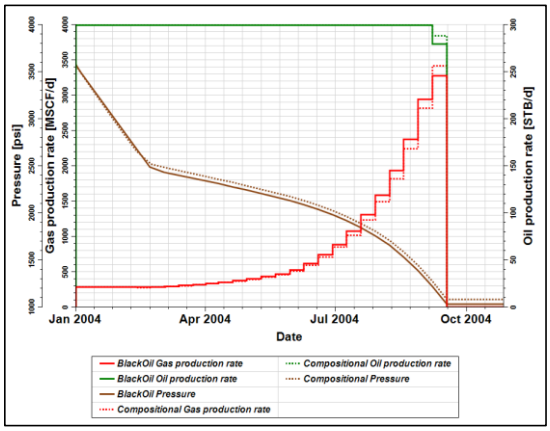

Figure 1: Production characteristics for the depletion strategy

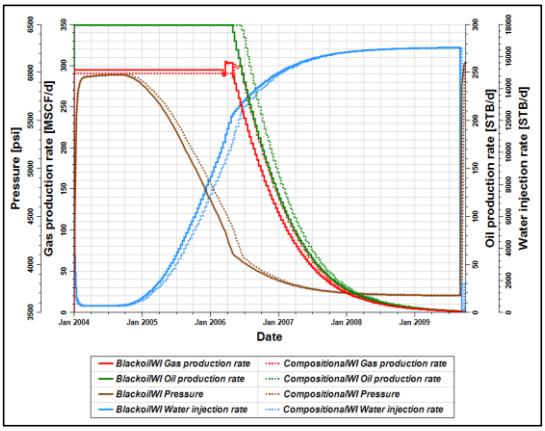

Figure 2: Production characteristics for the water imbibition strategy

In order to obtain a match between the black oil and compositional models for the gas injection strategy, it was necessary to avoid reaching miscible conditions during the simulation runs. We used an oil and light gas with a first miscible contact above reservoir conditions. The injection gas chosen was an equimolar mixture between CO_2 and C_1, and the final oil composition is displayed in *table 3*. As it can be seen in *fig.3*, we achieve a good match during the 10 years gas injection strategy for oil production, gas production, and reservoir pressure.

Component	Molar Weight	Overall composition
CO_2	44.01	0.015
N_2	28.013	0.008
C_1	16.043	0.186
C_2	30.07	0.029
C_3	44.097	0.07
C_4	58.124	0.078
C_5	72.151	0.06
C_{6+}	114.2	0.181
C_{9+}	170.3	0.161
C_{15+}	352.68	0.06
C_{21+}	422.8	0.089
C_{29+}	464.89	0.031
C_{36+}	563.08	0.032

Table 3: Compositional oil characteristics

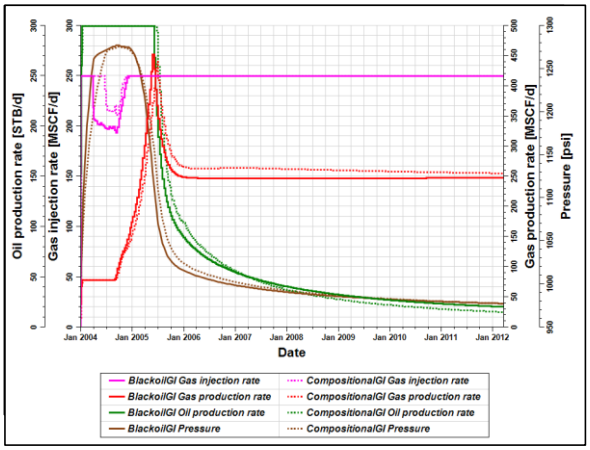

Figure 3: Production characteristics for the gas injection strategy

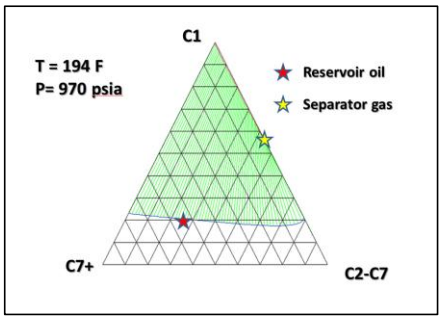

Figure 4: Ternary plot for the compositional oil

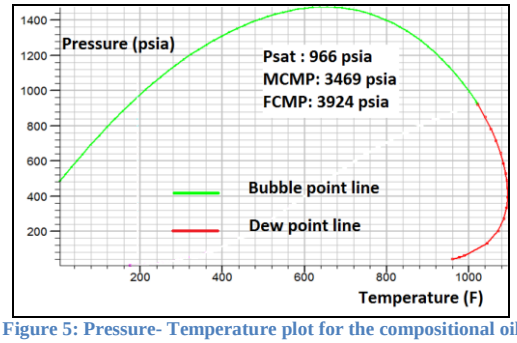

Figure 5: Pressure- Temperature plot for the compositional oil

WAG Strategy. FAWAG Strategy & Grid refining

Coarse models and WAG Strategy

The second step of this study was to define a consistent WAG strategy that would give the same production characteristics for the two simulators. This will enable us to make sure that any difference or variation between both models in the SAG strategy will come from the foam parameters of the model. This artificial strategy will especially focus on the gas breakthrough as we want to observe the foam effect and impact. Only one WAG cycle is performed, comprising one slug of water and one slug of gas; its characteristics are detailed in *table 4*. The model aims to depict a simple reservoir, with the first layer acting as a sealing cap. The layer 2 and 4 are very good reservoir zones, including a lower permeability zone in-between (layer 3). The two simulators provide us with a good match for oil production and gas production as seen in the figure below. The oil plateau rate is 10 years long and the gas breakthrough occurs after 5 years, which is soon enough to be sure to observe the delay caused by the foam injection

Comment [MAG1]: Check position of this title and next paragraph

WAG Strategy	
Strategy	1) Injection of water (1110 days) 2) Injection of Gas (3015 days)
Injection rate	1) 350 stb of water per day 2) 250 MScf of gas per day
BHP injection pressure	1300 pisa

Table 4: WAG Strategy

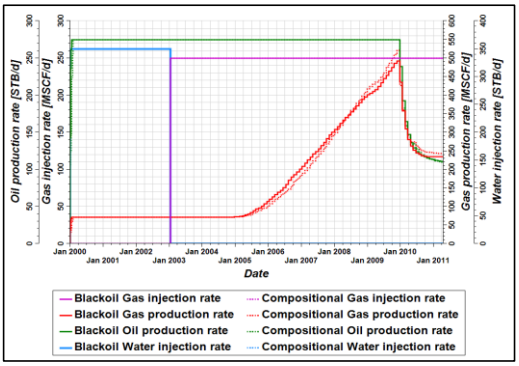

Figure 6: Production rate for the WAG strategy

Coarse Model	
Number of cells	750
(NX, NY, NZ)	(10, 15, 5)
Reservoir Dimensions	(1500 ft, 1000ft, 120 ft)
Pore Volume	6.2 MMrb
STOIIP	4.1 MMSTB
GIIP	1.07 MScf
WIIP	1.2 MMSTB
Time of simulation	4000 days
Distance between injector and producer	900 ft
Average horizontal permeability	280 mD
Average porosity	0.2
Vertical-horizontal permeability ratio	0.1
Datum depth	9200 ft
Top depth	9150 ft
Pressure at datum depth	970 psi
Oil production rate	300 stbd
production BHP	950 psia

Table 5 : Coarse Models characteristics

Layer	Porosity	Permeability	Thickness
Layer 1	8.7%	30 mD	20 ft
Layer2	25.9%	350 mD	30 ft
Layer 3	20%	200 mD	20 ft
Layer 4	25.9%	350 mD	30 ft
Layer 5	10%	70 mD	20 ft

Table 6: Properties in each layer

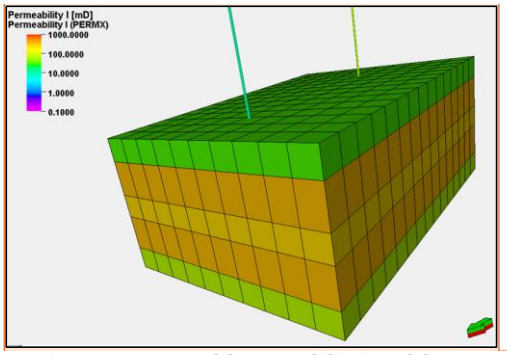

Figure 7: Coarse Model : permeability in each layer

Comment [SK2]: Cannot read the legend

SAG Strategy

The SAG strategy will be based on the previous WAG Strategy depicted in *table 4*, but it will include foam surfactants in the water. The model used will be the same as previously, and the main characteristics are described in *table 5*. Our simulators enable the surfactant to transform into foam when the gas comes into contact with the water containing the foam surfactant. Then, the foam effect is to reduce the gas mobility by a reduction factor M_{rf} as described in the first part of the study.

In the blackoil simulator, the foam surfactant is a tracer, and has neither mass nor viscosity. For the compositional simulator, we choose a surfactant with a molecular weight of 200 g/mol and a viscosity of 30 cp. For the base case, M_r, F_w, F_o, F_c will be kept constant and equal to 1. Concerning the function of surfactant concentration F_{sc}, C_s^r =0.0000075 mol fraction (0.03 lbm/stb) and C_s = 0.6 lbm/stb. The foam surfactant will be continuously injected during the water injection to ensure a constant foam concentration everywhere in the reservoir.

Grid refinement

Starting from a coarse grid of 750 cells, with the SAG strategy, a refinement has been processed, to measure the influence of the grid size. Especially, we focused on the gas production rate profile, which seems to be the most sensitive with grid size. A first conclusion of this study is that the SAG process is very sensitive to the gravity segregation, and needs a very detailed

model to fully capture the reservoir dynamics, which means a high number of cells in the vertical direction. At our scale, with a simple model, we need a cell height of 1.5 feet in average which results in a model with 256 times more active cells than the initial coarse model. This big amount of cells combined with the presence of foam, which implies new non-linear equations, means that the simulations of this study and those related will be very time-consuming.

Model Name	NX	NY	NZ	DX (ft)	DY (ft)	DZ (ft)	Number of cells
Coarse Model	10	15	5	100	100	25 (average)	750

Table 7: Coarse grid characteristics

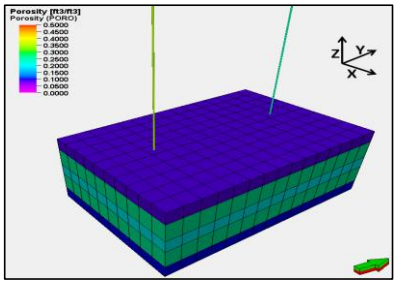

Figure 8: Porosity of the coarse model

The effect of the numerical dispersion is notable, as seen in *fig.9.* Numerically, We consider that the breakthrough occurs when the gas production rate is 1% higher than the gas production plateau rate. In the coarse grid, the breakthrough time occurs after 2715 days and 2714 days respectively, and for the fine grid, it occurs after 2139 days and 2204 days respectively.

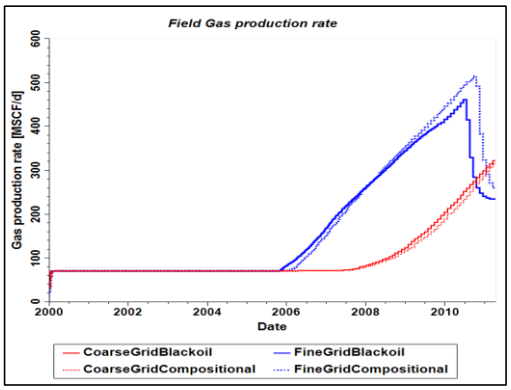

Figure 9: Effect of numerical dispersion: difference of gas production rate between the coarse grid and the fine grid

Fine Grid

Finally, our model will have the same reservoir characteristics and WAG strategy as described in *table 4*, but the water contains the foam surfactant (SAG strategy) and the grid is finer.

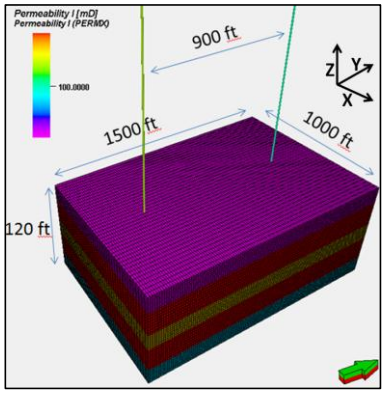

Figure 10: Permeability for the fine grid

Fine Grid & SAG strategy characteristics	
Number of cells	192 000
(NX, NY, NZ)	(40, 120, 40)
(DX, DY, DZ) (avg, in feet)	(25, 12.5, 3)
C_s^r	0.023 lbm/stb
C_s	0.6 lbm/stb

Table 8: Final Grid & FAWAG strategy characteristics

Base Case production profile

The production profile of the base case is displayed in *fig. 11*. For the rest of the study, we will consider that the breakthrough time is achieved when the gas production is more than 1% higher than the gas plateau rate production. In the blackoil base case, the gas breakthrough occurs after 2139 days and for the compositional base case, it occurs after 2204 days.

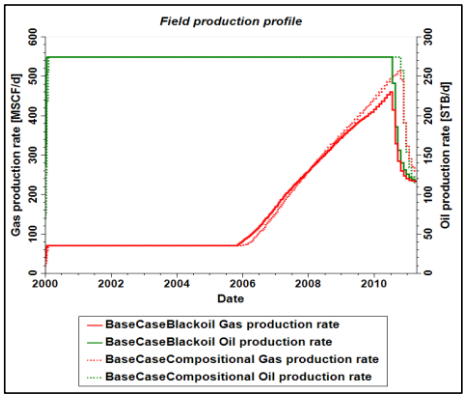

Figure 11: Gas and oil production profile for the base case and the fine grid

Sensitivities

This part of this study investigates the influence of each foam parameter on our model. As a consequence, the further steps of the study will rely on the analysis on the breakthrough time of each case, so we will extract the curve of the breakthrough time as a function of each foam parameter. As a matter of fact, with the base case, there is already a slight difference of breakthrough time between the blackoil and compositional simulators. This difference is negligible compared to the field's life, being only 100 days out of a 12 years simulation. But, as we will focus on this breakthrough time we need to normalize the breakthrough time curves, because plotting a relative breakthrough time instead of an absolute breakthrough time will enable us to get rid of the initial difference of breakthrough time and focus on the effective influence of our parameters. The normalization will consist in dividing by a breakthrough time reference. This breakthrough time reference won't always be the same, and will generally be the breakthrough time where there is a good stability.

Influence of the oil concentration factor F_o

As seen in *Eq. (4)*, the oil concentration factor $\boldsymbol{F_o}$ is a function of S_o, S_o^r and e_o. We make S_o^r and e_o vary, as seen in *fig.12* and *fig.13*. The absolute breakthrough time as a function of S_o^r for different e_o is displayed in *fig. 14*.

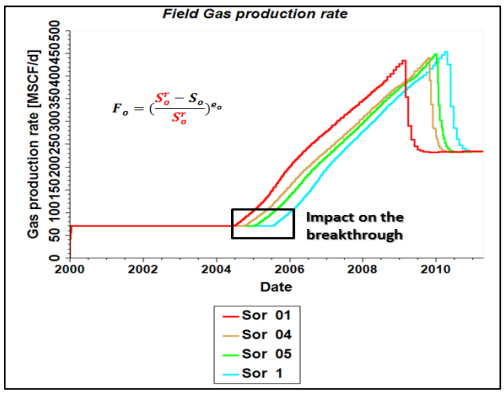

Figure 12: Gas production rate for S_o^r=0.1;0.4;0.5;1 for the blackoil case

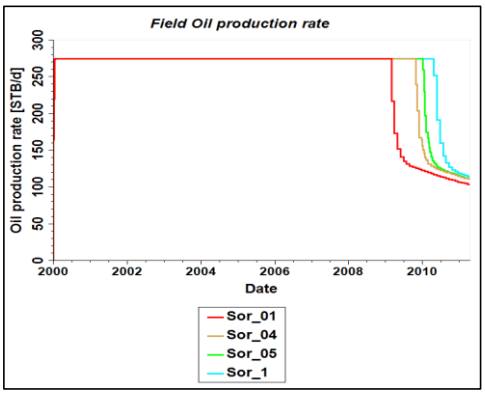

Figure 13: Corresponding oil production rate for S_o^r=0.1;0.4;0.5;1 for the blackoil case

Below $S_{o,res}$ = (0.2) the reference oil saturation has no impact on the breakthrough delay, and the breakthrough time occurs after 1659 days and 1754 days for the blackoil and compositional model respectively. These values of the breakthrough time have been used for the normalization of the curves, and the relative breakthrough time as a function of S_o^r is displayed in *fig.14*. The more effective the foam is, (high S_o^r and e_o), the higher the breakthrough delay is. A good match between both simulators is kept all along, which implies that S_o^r and e_o have the same impact on both simulators.

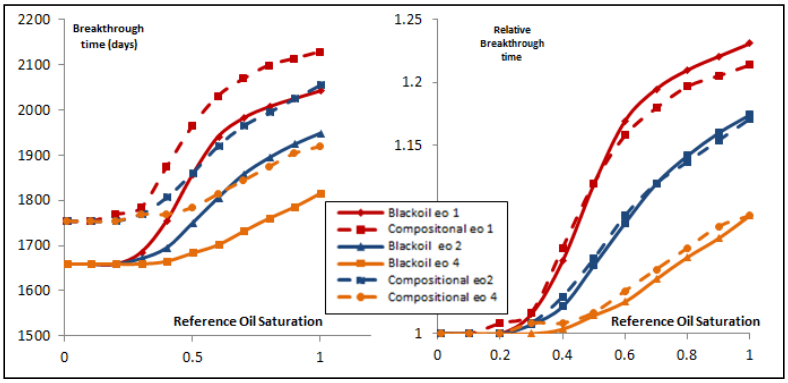

Figure 14: Breakthrough time and relative breakthrough time as a function of S_o^r. The right hand curve is normalized by the breakthrough time at $S_o^r = S_{o,res} = 0.2$

Influence of the water concentration factor F_w

As seen in *Eq. (3)*, the water concentration factor F_w is a function of S_w, S_w^r and f_w. The value of breakthrough delay when $S_w{}^r = S_{wc} = 0.2$ will be chosen as the reference for normalization. We have processed a sensitivity analysis for $S_w{}^r$ varying from 0 to 1 and with 3 values of f_w: 1, 10 and 50. As expected, the higher $S_w{}^r$ is, the lower the effect of the foam is, and the smaller breakthrough delay we have, as displayed in *fig.15*. The influence on the recovery factor confirms this trend and gives a good match between the two simulators. The range of breakthrough times for $S_w{}^r$ varying from 0 to 1 and the three values of f_w goes from 1671 days to 2121 days for the blackoil simulator, and from 1769 days to 2204 days for the compositional case.

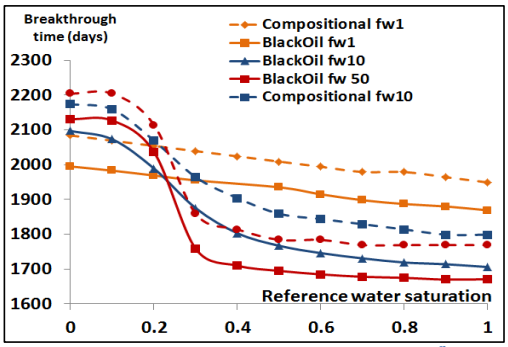

Figure 15: Breakthrough time as a function of $S_w{}^r$.

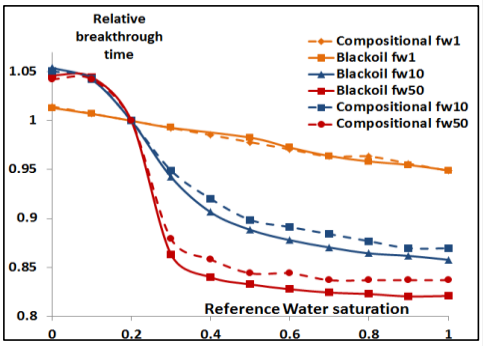

Figure 16: Relative breakthrough time as a function of $S_w{}^r$. The graph is normalized by the breakthrough time at $S_w{}^r = S_{wc} = 0.2$

Influence of foam concentration

In this part, we analyse the influence of the foam concentration on our model. In the same conditions and with the same SAG strategy, we evaluate the breakthrough time versus the surfactant concentration, as seen in *fig.17*.

We have chosen a range of surfactant concentration going from 0.0003 lbm/stb to 200 lbm/stb of foam surfactant. For the blackoil simulator, above 36 lbm/stb the concentration is too high and the pressure highly increases in the reservoir: we are unable to produce oil or gas with the initial injection pressure. This phenomenon occurs above 50 lbm/stb for the compositional simulator.

At very small concentration of foam, the breakthrough for the blackoil simulator occurs after 1659 days and for the

compositional simulator after 1754 days, which is exactly the respective breakthrough time of the blackoil and compositional simulator WAG strategy, so we can conclude that the foam has no effect here. These breakthrough times will enable us to normalize the curve, to have a relative breakthrough time, which is relative to the case without foam.

At low foam concentration we can see that the models match well with each other and the shape of the curve is the same, so the foam has a comparable effect on them, as seen in *fig. 18*. After 0.6 lbm/stb, differences appear between both simulators, and foam seems less effective for the compositional model.

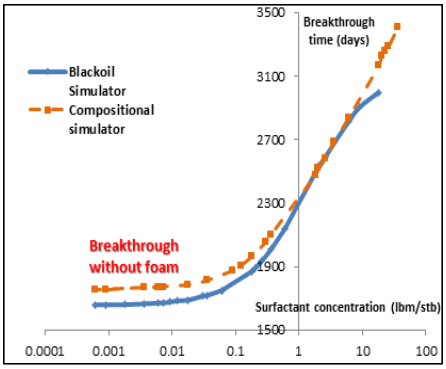

Figure 17: Breakthrough time as a function of the surfactant concentration

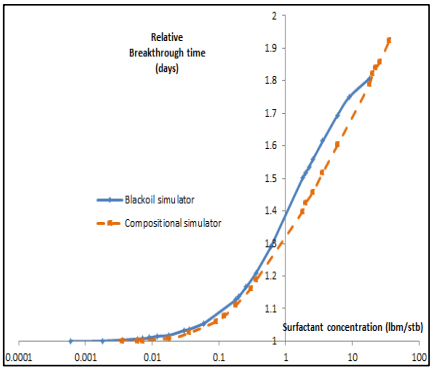

Figure 18: Relative breakthrough time, normalized by the breakthrough time without foam

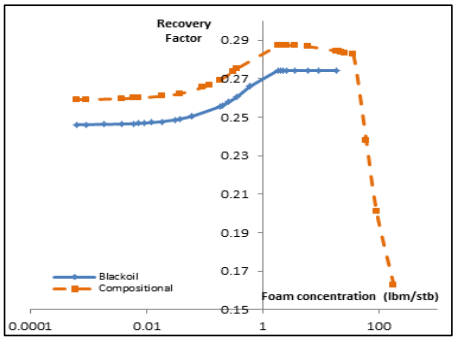

Figure 19: Recovery factor as a function of foam concentration

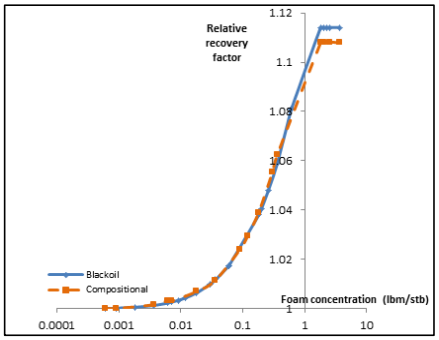

Figure 20: Relative recovery factor, normalized by the recovery factor without foam, as a function of foam concentration

Influence of the surfactant concentration factor F_{sc}

In this part, we investigate the impact of C_s^r and e_s on the breakthrough as parameter of the surfactant concentration factor F_{sc}. The influence of the surfactant concentration factor was investigated for the case where C_s = 0.6 lbm/stb and F_{sc} was modified by changing C_s^r and e_s. In *fig.21*, the breakthrough time versus C_s^r for three different values of e_s is displayed.

The range of breakthrough achieved for C_s and C_s^r is going from 1659 days to 2997 days for the blackoil simulator and from 1754 days to 3404 days for the compositional simulator. When $C_s^r \gg C_s$, the breakthrough time is stabilised at 1659 days and 1754 days respectively, we use these values of breakthrough time to normalize the breakthrough time, and the relative breakthrough time as a function of C_s^r is displayed in *fig.22.*

As seen in the figure, once normalized, the more effective the foam is (C_s^r low and e_s high), the bigger the difference is, which is consistent with the previous study. If the foam is too effective, the reservoir is unable to produce under these conditions because the reservoir pressure goes too high, as seen in *fig 19.*, with es=1, nothing is produced when C_s^r<0.01 lbm/stb, and when es=7, nothing is produced when C_s^r<0.5 lbm/stb.

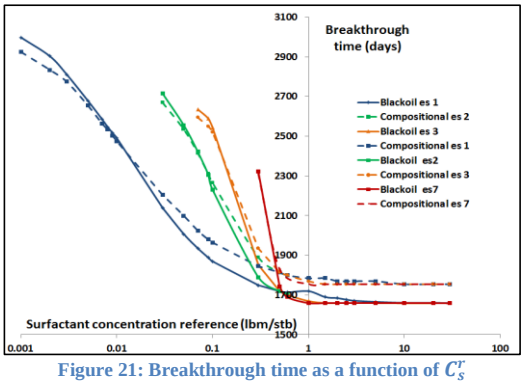

Figure 21: Breakthrough time as a function of C_s^r

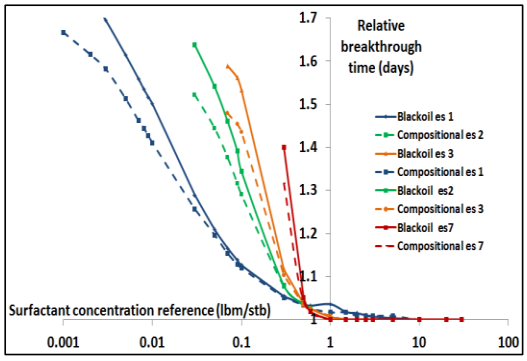

Figure 22: Relative breakthrough time, normalized by the breakthrough time without foam as a function of C_s^r

Influence of the reference mobility reduction M_r

M_r has a direct impact on foam efficiency, as it is a functional coefficient that will give more or less strength to the gas reduction factor.

With M_r varying between 0.01 and 50, the breakthrough time is between 1670 days and 3000 days for the blackoil case and between 1769 days and 2924 days for the compositional one. The lowest values of M_r are more stable, so the breakthrough time reference of 1670 days and 1769 days will be chosen as a reference for the blackoil and compositional simulator respectively. The corresponding recovery factor will be used to obtain the relative recovery factor curves. The relative breakthrough time the relative recovery factor as a function of M_r is displayed in *fig. 23*.

If $M_r < 1$, we obtain a good match for relative breakthrough time between both simulators.

If $M_r > 1$, both simulators differ and the blackoil foam is more effective than the compositional foam. The blackoil simulator has until 20 point of percentage more effect on the breakthrough time than our compositional simulator. But this difference of breakthrough time has not much impact of the recovery factor, as the difference is less than 5 points of percentage at maximum.

If M_r is too high (more than 50), then the pressure needed at the injector is too high and we are unable to produce, which explains why the recovery factor decreases when $M_r > 1$.

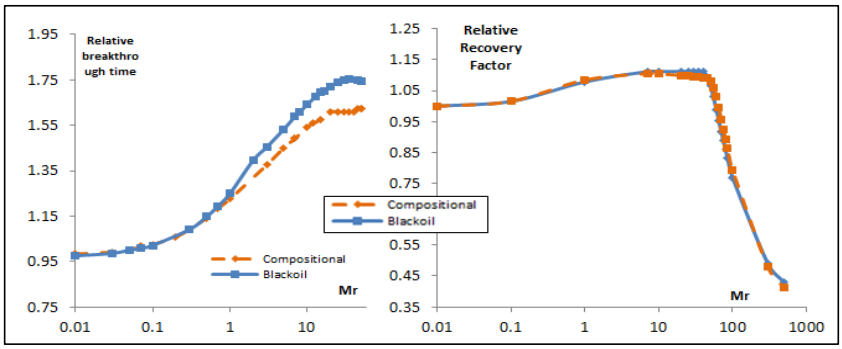

Figure 23: Relative Breakthrough time and relative recovery as a function of M_r. The curves are normalized with the breakthrough time reached when $M_r \rightarrow 0$

Influence of the capillary number reduction factor Fc

The capillary number gives a quantitative value of the ratio between shear forces and capillary forces. A general expression for this capillarity number is

$$N_c = \frac{u_p \mu_p}{\sigma_{pq}} \quad \text{(8)}$$

In each cell, when including the Darcy's law for a single phase, it becomes

$$N_c = \frac{C_N}{C_D}\left\|\frac{T\,\Delta P_p}{A}\right\|\frac{1}{\sigma_{pq}} = C_N.\frac{\|K.\nabla P_p\|}{\sigma_{pq}} \quad (9)$$

Here, only the blackoil cased is displayed because both simulators lead to similar conclusions and the normalization process was complex. The range of breakthrough time achieved is more than 1200 days with reference capillary number going from 1.10^{-9} to 5.10^{-7} and the exponent going from 1 to 3. When this parameter is too high, and causes a breakthrough time superior to 3000 days, we have reached the limit of the foam and the well does not produce anymore. This means that the higher the capillary number is, the less effective the foam is.

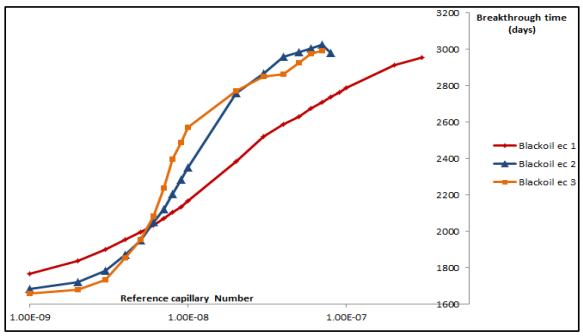

Figure 24: Breakthrough time as a function of N_c^r for the blackoil simulator

Influence of the foam decay

The decay comes from an alteration of the characteristics of the foam with time. The decay model is different in both simulators. In the blackoil simulator, foam, which was considered as a tracer, simply disappears as the time goes by. The disappearance is modelled with an exponential decay law with a given half-life $t_{1/2}$, depending on the oil and water saturation.

$$\frac{d[Foam]}{dt} = -\frac{\ln(2)}{t_{1/2_{ads,blackoil}}(S_o,S_w)}.[Foam] \quad (10)$$

In the compositional simulator, foam is not considered as a tracer, but has a physical mass and volume. The disappearance is also modelled with a chemical transformation, foam becoming water.

$$Foam \rightarrow Water$$

The reaction rate R_r is given by an Arrhenius equation:

$$-\frac{d[Foam]}{dt} = R_r = A_{r_{compositional}} e^{-E_r/RT}[Foam]^{n_{foam}} \quad (11)$$

To calibrate both simulators and simulate similar decay behaviours, we need to match both equations above. We also chose a simple case, where $t_{1/2_{ads,blackoil}}$ does not depend on the oil and water saturation, A_r is constant, E_r is null and the order of the reaction is n_{foam}.

Then for the blackoil case,

$$\frac{d[Foam]}{dt} = -\frac{\ln(2)}{t_{1/2_{ads,blackoil}}}.[Foam] \quad (12)$$

And for the compositional case,

$$\frac{d[Foam]}{dt} = -A_{r_{compositional}}[Foam]^{n_{foam}} \quad (13)$$

Then,

$$A_{r_{compositional}} = \frac{\ln(2)}{t_{1/2_{ads,blackoil}}}.[Foam]^{n_{foam}-1} \quad (14)$$

Which implies that the reaction order has also to be $2n_{foam} - 1$.

The only consistent calibration respects

Comment [MAG3]: Check equation

$$2n_{foam} - 1 = 2n_{foam} \quad (15)$$

$$n_{foam} = 1 \quad (16)$$

To calibrate both simulators, the order of the reaction has also to be 1

$$\frac{d[Foam]}{dt} = -A_{r_{compositional}}[Foam] \quad (17)$$

Then the calibration is given by,

$$A_{r_{compositional}} = \frac{\ln(2)}{t_{1/2_{blackoil}}} \quad (18)$$

This can lead to two kinds of results, as seen in *fig. 25*. If the foam decay rate is less than $0.0001\ days^{-1}$, then the decay process is too slow and the breakthrough time obtained is the same as the base case : the breakthrough occurs after 2139 days and 2204 days for black oil and compositional respectively.

If the decay rate is higher than $0.01\ days^{-1}$ then the decay rate is so quick that the foam disappears as soon as it appears. The breakthrough occurs after 1659 days and 1754 days for black oil and compositional respectively, same breakthrough time as in the WAG base case.

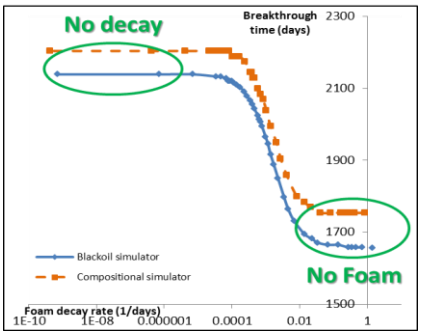

Figure 25: Breakthrough time as a function of the foam decay rate

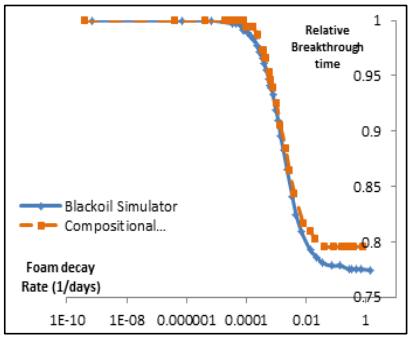

Figure 26: Relative breakthrough time, normalized by the breakthrough time at low foam decay rate, as a function of the foam decay rate

Influence of the foam adsorption

The adsorption comes from an interaction between the surrounding rock and the foam. This contact results in an adhesion of one part of the foam molecules, making them inactive. Also, this process mainly depends on the foam concentration and on the rock properties. In the blackoil simulator, a given concentration of foam tracer will become solid instantaneously. This transformation depends on the foam tracer concentration and the rock adsorption capacity C_{aeq} (how much foam a given mass of rock is able to adsorb).

In the compositional simulator, adsorption can be modelled with a reaction, similar to the decay reaction. The reactant will be the foam, and the product will be the solid, which will have the same characteristics of our foam (viscosity, molar mass…)

$$Foam \rightarrow Solid$$

An equilibrium deviation term can be used to model deviation from our equilibrium state. The reaction rate R_r will be multiplied by d where

$$\mathbf{d} = \boldsymbol{\theta}.(\mathbf{C_{aeq}} - \mathbf{C_a}) \quad (19)$$

Here, the half-life for $C_{aeq} - C_a$ will be

$$t_{1/2_{adsorption,compositional}} = \frac{ln(2)}{B_{r_{compositional}}} \quad (20)$$

Where $B_{r_{compositional}}$ is the reaction rate constant

In fig. *27* and *fig. 28* the breakthrough time and the relative breakthrough time have been plotted as a function of the rock adsorption rate, for different reaction rates. When the adsorption rate is less than 1.10^{-6} lbm/lbm, the breakthrough time for

the compositional and blackoil simulator are respectively 2204 days and 2139 days, which are the same breakthrough time as our base case: there is no adsorption below 1.10^{-6} lbm/lbm. We will use these breakthrough times to normalize the curves. As for the decay study, when the adsorption rate is higher than 1 lbm/lbm, the adsorption phenomenon has made all the foam disappear so quickly, that the breakthrough time is the same as without foam. The obtained breakthrough times are 1659 days and 1714 days for the blackoil and compositional simulator.

For the blackoil case, the adsorption is instantaneous. For the compositional case, there is an adsorption reaction, which includes a reaction rate. We obtain a match between the compositional and the blackoil case, if the reaction rate is higher than 1000 $days^{-1}$. Above this rate, the reaction is almost instantaneous at the simulation scale and the match is possible. As for the decay, the match is only achieved in range of adsorption rates, going from 1.10^{-6} lbm/lbm to 1.10^{-3} lbm/lbm, because the variation of the adsorption rate implies a variation of foam concentration, and there can only be a good match between both simulators in a reasonable range of foam concentration.

As a conclusion, a match is possible between the blackoil instantaneous model and the compositional model, if we create reactions quick enough to be seen as instantaneous. Two issues are raised with this calibration. First of all, the adsorption process takes time, and the compositional model is more accurate, as an instantaneous reaction is non-physical. For this reason, when adsorption is included in a model, it is better to use the compositional simulator that will give a better picture of the physics behind the adsorption phenomenon. Second of all, increasing the reaction rate creates convergence problems in the model. It increases highly the simulation time, and for extreme cases, the simulation doesn't even run. That was the case for our compositional simulation depicted above, with a reaction rate of 100 000 $days^{-1}$ and an adsorption rate superior to 1.10^{-4} lbm/lbm.

Comment [MAG4]: In discussion (at end)?

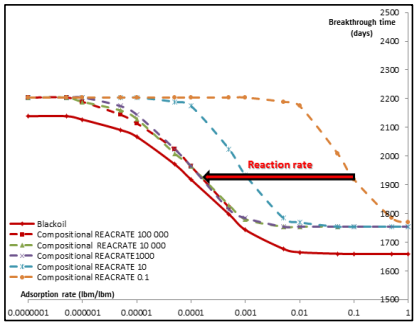

Figure 27: Breakthrough time as a function of the adsorption rate. The Compositional simulator comprises different reaction rate, going from 0.1 $days^{-1}$ to 100 000 $days^{-1}$

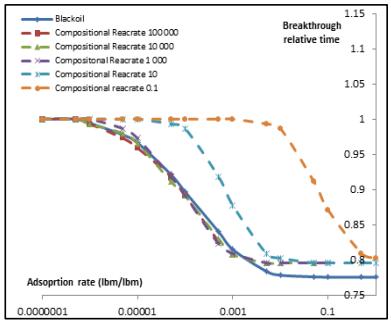

Figure 28: Relative breakthrough time as a function of adsorption rate. The curves are normalized by the breakthrough time at low adsorption rate

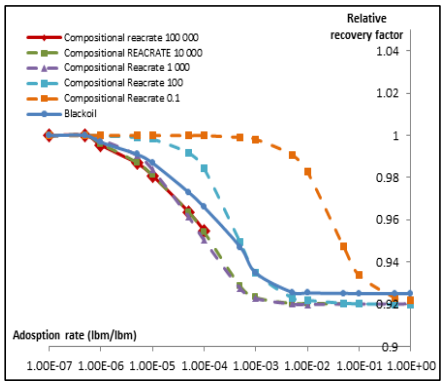

Figure 29: Relative recovery factor as a function of adsorption rate. The curves are normalized by the recovery factor at low adsorption rate

Discussion

This work has been an extension of the studies from Cheng (2000), Aarra (2002), Shan (2004), Spirov (2012) and Rossen (2013), who have widely investigated the physics behind the blackoil simulator. Our results from the black oil simulator are consistent with the behaviour reported in the literature, with regard to the surfactant concentration factor F_{sc}, the water reduction factor F_w, the oil reduction factor F_o, or the capillary number reduction factor F_c.

We have compared the blackoil simulator with the compositional simulator and shown that comparable results are obtained when decay and adsorption are ignored. We have introduced chemical reactions in the compositional model to represent decay and adsorption, and we have been able to depict the difference in mechanistic characteristics, compared to the black oil representation.

Gas injection has been the cornerstone for a good SAG match between the compositional and blackoil simulators. In the blackoil model, the injection gas is immiscible. In the compositional simulator, the injection gas used is composed of 50 % of C_1 and 50 % of CO_2. The different of gas injection process explains why both simulator models don't match when foam is highly efficient ($\frac{C_s}{C_s^r} > 100$ or M_r>5). At high foam concentration, the gas is slowed down and penetrates slowly into the pores. Because the gas is less mobile, it is more likely to interact with the reservoir oil, and difference in miscibility properties will have a bigger impact on the production.

Another conclusion of this study is that the FAWAG process is very sensitive to the gravity segregation, and needs a very detailed model to fully capture the reservoir dynamics, which means a high number of cells. At our scale, with a really simple model, we need a cell height of 1.5 feet in average which results in a model with 256 times more active cells than the initial coarse model. This big amount of cells combined with the presence of foam, which implies new non-linear equations, means that the simulations of this study and those related will be very time-consuming.

As we focused on the breakthrough time in our study, which is slightly different in the base case with a difference of 100 days between the two simulators, normalization has been necessary in the sensitivity study. This normalization enabled us to compare the evolution of the breakthrough time and recovery factor when changing a foam parameter. The normalization process has been based on a ratio between the actual breakthrough time and a reference breakthrough time. In each case, the rule to determine the reference breakthrough time has been to look into stabilization of the breakthrough time curve as a function of the foam parameter and pick the extreme value of breakthrough time of the plateau.

Concerning the adsorption process, in the blackoil simulator, the transformation of foam into solid is described as instantaneous. In the compositional simulator, it is a real reaction that takes times and involves a reaction rate. The only way to obtain a good match between both simulators is to choose a reaction rate high enough to simulate an instantaneous reaction.

For the adsorption and decay, the fact that a perfect match is not achieved between both simulators for the relative breakthrough time is normal. As the foam decay rate varies in the model, the effective foam composition varies as well in the reservoir. As seen previously, there is not a perfect match between both simulators for the breakthrough relative time when the foam composition changes, and for this reason we could not expect a match for both simulators on such a wide range of foam decay rate.

Conclusions

Based on the comparison between the blackoil simulator and the compositional simulator:

1. The decay and adsorption process cannot be ignored when dealing with a foam process, as this can lead to a complete disappearance of the reservoir foam.
2. The compositional simulator depicts better the reality when including adsorption, as it includes reactions which have physical transformation times.
3. Decay models can be matched in both simulators as soon as the reaction order is 1 in the compositional simulator.
4. The FAWAG process is very sensitive to the grid size, and especially in the vertical direction, due to the gravity segregation phenomenon.
5. The impact of each foam parameter on the recovery factor is important, and the difference between simulators stay relatively small compared to that.
6. The most influent parameters on the breakthrough, and therefore recovery factor are the reference mobility reduction M_r , the surfactant concentration function F_{sc} and the capillary number fuction F_c.
7. S_o^r (reference oil saturation), e_o (foam strength dependency on oil), S_w^r (reference water saturation), f_w (foam strength dependency on water), N_c^r (reference capillary number), and e_c (foam strength dependency on capillary number) have the same influence on the blackoil and compositional simulator
8. $\frac{C_s}{C_s^r}$ (ratio between the surfactant concentration and the reference surfactant concentration) and M_r (reference mobility reduction) have the same influence on both model if foam is not to concentrated or too effective. In such a case, the blackoil gives higher breakthrough delays.

9. A good correlation between two models, a blackoil simulator and a compositional simulator, is hard to achieve when injecting gas. In this case, it is preferable to use the compositional simulator which will take into account the miscibility component by component. Furthermore, the nature of the injected gas is better defined as the composition. of the gas can be selected. In the black oil simulator, the injected gas has to be the one that comes out of the separator.
10. Some very specific condition need to be combined to have a good WAG match between both simulators. The oil needs to be heavy enough to have a high multicontact miscibility and first miscibility pressure at reservoir conditions. The injection process should be smooth enough to avoid the reservoir pressure to stay far under the miscibility pressure
11. If foam is too efficient (C_s too high, C_s^r too low, $M_r$too high), then the injector pressure needed is too high when the foam is formed and there will be no positive improvement in production

Recommendations for Further Study

To improve the accuracy and the range of validity of this study:

1. Comparison with real measurements from the field would help to validate these conclusions.
2. More sensitivity studies on the composition of the injection gas are needed. In particular, recommendations on when the black oil model is valid for a given gas composition, would help engineers in selection of the appropriate model
3. More study of the effects of upscaling is needed: for example, the reaction rates for adsorption and decay may need to be adjusted at different scales.
4. More sensitivity on the vertical grid refinement should be done to better understand the numerical dispersion.

Nomenclature

cp	Centipoise
Fig.	Figure
ft	Foot
lb	Pound (mass unit)
mD	Milli-darcy
p	Pressure (psi)
psi	Pounds mass per square inch
R_s	Solution gas ratio (Mscf/stb)
scf	Standard cubic foot
S_g	Gas saturation
S_o	Oil saturation
S_{oc}	Critical oil saturation
S_{or}	Residual oil saturation
S_{wc}	Connate water saturation
stb	Stock-tank barrel
M_r	Reference mobility reduction
F_{sc}	Function of surfactant concentration
F_w:	Function of water concentration
F_o	Function of oil concentration
F_c:	Function of capillary number
C_s	Active foam concentration
C_s^r	Reference concentration
e_s	Foam strength dependency of surfactant concentration
f_w	Weighting factor (controls the sharpness in the change in mobility)
S_w	Water saturation
$S_w{}^r$	Reference water saturation
S_o^r	Reference oil saturation
S_o	Reference oil saturation
e_o	Foam strength dependency on oil saturation
N_c^r	Reference capillary number
N_c	Capillary number
e_c	Foam strength dependency on capillary number
$q_{g,no\ foam}$	Gas rate without foam in the reservoir
λ_g	Mobility
$q_{g,foam}$	Gas rate with foam in the reservoir
P	Reservoir pressure
NX	Number of cells in the X direction
NY	Number of cells in the Y direction
NZ	Number of cells in the Z direction
DX	Number of cells in the X direction
DY	Number of cells in the Y direction
DZ	Number of cells in the Z direction
$STOIIP$	Stock tank of oil in place (stb)
$GIIP$	Gas in place (Mscf)
$WIIP$	Water in place (stb)
u_p	Velocity of the phase p
μ_p	Viscosity of the phase p
σ_{pq}	Surface tension between phase p and q
K	Absolute permeability
ΔP	Pressure gradient
σ_{wg}	Surface tension between water and gas
C_N	Unit conversion factor
T	Transmissibility
P_p	Phase potential
C_D	Darcy Constant
A	Cell boundary area
A_r	Reaction rate constant
E_r	Activation molar energy
n_{foam}	Reaction order of foam
R_r	Reaction rate
θ	Porosity
C_{aeq}	Equilibrium adsorbed solid concentration (if the reaction was instantaneous)
C_a	Actual adsorbed solid concentration

References

Aarra, M. G., Skauge, A. and Martinsen, H.A. 2002. FAWAG: A Breakthrough for EOR in the North Sea. *SPE J.* DOI: 10.2118/77695-MS

Abbaszadeh, M. and Ren, G. 2013. Sinulation Techniques for Surfactant Phase Behavior and Foam Flow Modeling in Fractured Reservoirs. *SPE J.* DOI: 10.2118/166032-MS

Alvarez, J. M., Rivas, H.J. and Rossen, W.R. 2001. Unified Model for Steady-State Foam Behavior at High and Low Foam Qualities. *SPE J.* DOI: 10.2118/74141-PA

Blaker, T., Celius, H. K., Lie, T., Martinsen, H. A., Rasmussen, L., & Vassenden, F. 1999. Foam for Gas Mobility Control in the Snorre Field: The FAWAG Project. *Society of Petroleum Engineers* DOI:10.2118/56478-MS

Cheng, L, Feme, A.B., Shan, D., Coomve, D.A. and Rossen, W.R. 2000. Simulating Foam Processes at High and Low Foam Qualities. *SPE J.* DOI: 10.2118/59287-MS

De Gennes, P.G., 1992. Soft matter. *CERN-VIDEO*-C-120-A,

De Gennes, Pierre-Gilles, Françoise Brochard-Wyart, and David Quéré.Capillarity and wetting phenomena: drops, bubbles, pearls, waves. *Springer*, 2004.

Farajzadeh, R., Andrianov, A., Krastev, R., Hirasaki, G. and Rossen, W.R. 2012 Foam-Oil Interaction in Porous Media: Implications for Foam Assisted Enhanced Oil Recovery. *SPE J.* DOI: 10.2118/154197-MS

Greenwalt, W.A, Vela, S., Christian, L.D. and Shirer, J.A. 1982. A field Test of Nitrogen WAG Injectivity. *SPE J.* DOI: 10.2118/8816-PA

Hanssen, J. E., Surguchev, L. M., & Svorstol, I. 1994. SAG Injection in a North Sea Stratified Reservoir: Flow Experiment and Simulation. *Society of Petroleum Engineers*. doi:10.2118/28847-MS

Holt, T., Vassenden, F., & Svorstol, I. 1996. Effects of Pressure on Foam Stability; Implications for Foam Screening. *Society of Petroleum Engineers*. doi:10.2118/35398-MS

Khatib, Z. I., Hirasaki, G. J., & Falls, A. H. 1988. Effects of Capillary Pressure on Coalescence and Phase Mobilities in Foams Flowing Through Porous Media. *Society of Petroleum Engineers*. doi:10.2118/15442-PA

Kovscek, A. R., Reservoir Simulation of Foam Displacement Processes, 1998 *UNITAR* 1998.186

Le, V.Q., Nguyen, Q. P. and Sanders, A. 2008. A Novel Foam Concept With CO2 Dissolved Surfactants. *SPE J.* DOI: 10.2118/113370-MS

Ma, K., Ren, G., Mateen, K., Morel, D. and Cordelier, P. 2014. Literature Review of Modeling Techniques for Foam Flow Through Porous Media. *SPE J.* DOI: 10.2118/169104-MS

Mannhardt, K., Novosad, J. J., & Jha, K. N. N. 1994. Adsorption of Foam-forming Surfactants In Berea Sandstone. *Petroleum Society of Canada*. doi:10.2118/94-02-04

Mannhardt, K., Novosad, J. J., & Schramm, L. L. 1998 Foam/Oil Interations at Reservoir Conditions. *Society of Petroleum Engineers* DOI:10.2118/39681-MS

Mysels, K. J. 1959. Soap films: studies of their thinning and a bibliography. *Pergamon press*.

Nguyen, Q. P., Alexandrov, A. V., Zitha, P. L., & Currie, P. K. 2000 Experimental and Modeling Studies on Foam in Porous Media: A Review. *Society of Petroleum Engineers*. DOI:10.2118/58799-MS

Rossen, W.R. 2013. Numerical Challenges in Foam Simulation: A Review. *SPE J.* DOI: 10.2118/166232-MS

Shan, D., and Rossen, W.R. 2004. Optimal Injection Strategies for Foam IOR . *SPE J.* DOI: 10.2118/88811-PA

Skauge, A., Aarra, M. G., Surguchev, L., Martinsen, H.A., and Rasmussen, L. 2002. Foam-assisted WAG: Experience from the Snorre Field. *SPE J.* DOI: 10.2118/75157-MS

Spirov, P., Rudyk, S. and Khan, A. 2012. Foam Assisted WAG, Snorre Revisit with New Foam Screening Model. *SPE J.* DOI: 10.2118/150829-MS

Svorstol, I, Vassendenm F. and Mannhardt, K. 1996. Laboratory Studies for Design of a Foam Pilot in the Snorre Field. *SPE J.* DOI: 10.2118/35400-MS

Appendix A: Literature Review

Table A-1: Key milestones related to this study

Paper n°	Year	Title	Authors	Contribution
Percamon Press. Inc.	1959	"Soap Films: studies of their thinning and a bibliography"	K.J. Mysels, K. Shinoda, S. Frankel	First complete description of soaps and surfactants effects, especially on surface tension
Science	1992	"Soft Matter"	P.G. De Gennes	Description of a broad range of physical matter, with interaction between surfaces
28847	1994	"SAG Injection in a North Sea Stratified Reservoir. Flow Experiment and Simulation"	J.E Hanssen, L.M. Surguchev, I. Svorstol	A study of a novel recovery process for stratified reservoirs with large permeability contrasts. A slug of foaming surfactant is injected alternately with gas, thus by analogy with WAG making this a SAG injection process.
35400	1996	"Laboratory Studies for Design of a Foam Pilot in the Snorre Field"	I. Svorstol, F. Vassenden, K. Mannhardt	This paper presents a summary of laboratory work carried out to support the design of a foam pilot in the North Sea Snorre Field.
35398	1996	"Effects of Pressure on Foam Stability; Implications of Foam Screening"	T. Holt, F. Vassenden, I. Svorstol	The stability of foam in porous media has been investigated by core flooding at pressures horn 10 to 300 bar, Mb in the presence and absence of oil.
59287	2000	"Simulating Foam Processes at High and Low Foam Qualities"	L. Cheng, A. B. Reme, D. Shan,† D. A. Coombe, W. R. Rossen	Foams used for gas or acid diversion exhibit two flow regimes, depending on foam quality. Two foam simulators, one the most widely used commercial foam simulator and the other, fit steady-state foam behavior in both regimes.
77695	2002	"FAWAG: A Breakthrough for EOR in the North Sea"	Aarra, M. G., Skauge, A. and Martinsen, H.A	Give the fitting parameters for the blackoil simulator in the Snorre field
Springer	2004	"Capillarity and Wetting Phenomena: Drops, Bubbles, Pearls, Waves"	P.G. De Gennes, F. Brochard-Wyart, David Quere	All about drops, bubbles, Pearls, Waves

150829	2012	"Foam Assisted WAG, Snorre Revisit with New Foam Screening Model"	Spirov, P., Rudyk, S. and Khan, A	Try to understand the field scale simulation model of Foam Assisted Water Alternating Gas that had been implemented to two Norwegian Reservoirs
166232	2013	"Numerical Challenges in Foam Simulation: A Review"	W. R. Rossen	Review challenges to accurate simulation of foam enhanced oil recovery, with a focus on numerical issues
169104	2014	Literature Review of Modeling Techniques for Foam Flow through Porous Media	K. Ma, G. Ren, K. Mateen, D. Morel, P. Cordelier	It reviews modeling approaches obtained from different publications for describing foam flow through porous media

SPE 35400 (1996)

Laboratory Studies for Design of a Foam Pilot in the Snorre Field

Authors: Svorstal, I. Vassenden, F. Mannhardt, K.

Contribution to the understanding of foam EOR processes: (*)

First to undertake laboratory tests on Snorre cores, to evaluate the gas blocking and mobility reduction of foam.

Objective of the paper:

Evaluate the gas blocking and mobility reduction of foam with core data.

Methodology used:

5 modes of corefloods were used in the foam experiments: Gas blocking, foam injection, gas injection, oil blocking, oil/foam coinjection.

Conclusion reached:

1. Apparent foam viscosity decreased with increasing gas fractional flow

2. Different foam rheology depending on the fractional flow. At low gas fractional flow, the foam in shear thinning, at drier fractional flow, there is no shear dependence

3. The level of oil saturation affected foam performance

4. Foam viscosity seems not to depend on the gas (true for three different gases)

5. A period of ageing of the core with surfactant seems necessary before the foam develops its maximum strength

6. A surfactant pre-flush appears to promote foam formation

7. Up to a certain imposed threshold pressure gradient, foam effectively blocked gas flow.

Comments:

No comments

SPE 59287 (2000)

Simulating Foam Processes at High and Low Foam Qualities

Authors: Cheng, L., Reme, A.B., Shan. D., Coombe, D. A., Rossen, W. R.

Contribution to the understanding of foam EOR processes: (*)

Simple procedure for fitting simulator parameters to a set of steady-state foam behavior in both regimes.

Objective of the paper:

1. Describe a methodology for fitting simulator parameters to a set of steady-state foam behavior in both regimes
2. Apply this methodology to new data.

Methodology used:

Conclusion reached:

1. Two foam-simulation algorithms (UTCOMP and STARS), fit foam behavior in both the high and low quality foam-flow regines reasonably well

2. A simple scheme for fitting the parameters in both models is presented

3. Necessity of using data from low and high quality regime to fit foam behavior (otherwise, incorrect trends)

4. Shear thinning can increase foam injectivity if foam is injected in the low quality regime

Comments:

No comments

SPE 77695 (2002)

FAWAG: A Breakthrough for EOR in the North Sea

Authors: Aarra, M. G., Skauge, A. and Martinsen,

Contribution to the understanding of foam EOR processes: (*)

Give the fitting parameters for the blackoil simulator in the Snorre field

Objective of the paper:

1. History match has been done using a commercial foam simulator
2. Evaluate further potential for FAWAG in the Snorre Field

Methodology used:

History match with a commercial foam simulator

Conclusion reached:

1. Foam simulation in agreement with other estimates and confirm a reduced GOR and additional oil recovery
2. Effect of foam has been shown to last over a long duration and the breakdown of foam is captured in the simulations
3. Indication of a significant potential for increased oil production and storage of gas.
4. Further use of foam to improve gas sweep on the Snorre field is recommended

Comments:

No comments

SPE 150829 (2012)

Foam Assisted WAG, Snorre Revisit with New Foam Screening Model

Authors: Spirov, P., Rudyk, S. and Khan, A,

Contribution to the understanding of foam EOR processes: (*)

Try to understand the field scale simulation model of Foam Assisted Water Alternating Gas that had been implemented to two Norwegian Reservoirs

Objective of the paper:

1. Check the authenticity of presented new foam model in commercial software
2. Suggest some improvement for the simulation software

Methodology used:

History match with a commercial foam simulator, simulation studies and sensitivity process

Conclusion reached:

1. Multiple MRF's should be use for different foam cycles rather than one single value
2. MRF should be made pressure dependent
3. Include Mrf, FSO and FSW in schedule well section

Comments:

No comments

SPE 166232 (2013)

Numerical Challenges in Foam Simulation: a review

Authors: Rossen, W. R.

Contribution to the understanding of foam EOR processes: (*)

Not much: it is a review of previous literature

Objective of the paper:

Review challenges to accurate simulation of foam enhanced oil recovery, with a focus on numerical issues

Methodology used:

Collect and review the numerical challenges to foam simulation. Measurement of the impact of these parameters on final recovery. Discuss the origin of the challenges how to recognize them, how they can be mitigated, and whether they arise from a correct representation of foam physics.

Conclusion reached:

1. Several effects of water saturation: abrupt change in gas mobility with water saturation, fluctuation in injectivity and mobility due to finite-difference simulations (large variation of saturation in each block). Solution: Refining the grid near the well and at the foam front.

2. Several effects of surfactants concentration: Numerical dispersion of the surfactant front can be significant. Replacing the dependence on surfactant concentration with a step function introduces fluctuations in fluxes at each successive grid block. Solution: refining the grid in both cases

3. Several effects of oil saturation: successive grid blocks may lie on opposite sides of a boundary between a strong and weak foam.

Comments:

No comments

SPE 16032 (2013)

Simulation Techniques for Surfactant Phase Behavior and Foam Flow Modeling in Fractured Reservoirs

Authors: Maghsood Abbaszadeh

Contribution to the understanding of foam EOR processes: (*)

Provide with an innovative method to describe simulate foam flow combined with the complex chemical process of surfactant injection in naturally fractured systems.

Objective of the paper:

Modeling surfactant phase behavior as a function of salinity and representing micro emulsions properties. Challenging because commercial simulators lack the capability to explicitly model these complex chemical processes.

Methodology used:

Based on the fundamental idea that foam flow is primarily restricted to the fracture network and the surfactant is transported into matrix where the intended chemical EOR processes occur. The problem at hand is decomposed into two parts of modeling foam flow in fractures and modeling surfactant flow in matrix. The matrix will be defined as a system with a viscosity of set 1, and the fracture a system with a viscosity of set 2. The viscosity of set 1 (matrix) is described by ME viscosity of chemical EOR, while viscosity of set 2 (fractures) is controlled by foam apparent viscosity.

Conclusion reached:

1. Innovative techniques have been developed for fractured reservoirs to simulate micro emulsions phase behavior in matrix and foam mobility control in fracture using commercial compositional CMG-STARS

2. Foam flow is primarily restricted to the fracture system and surfactant chemical EOR occurs mainly in matrix. Thus the problem is decomposed to proper modeling of foam flow in fractures and surfactant micro emulsions processes in matrix.

3. The techniques developed provide a methodology for modeling foam surfactant chemical EORE in naturally fractured reservoirs, accounting for both complex phase behavior of micro emulsions and foam flow by manipulating a publicly available commercial simulator without resorting to in-house or inaccessible specific simulators.

Comments:

No comments

SPE 113370 (2008)

A Novel Foam Concept with CO_2 Dissolved Surfactants

Authors: Viet Q. Le, Quoc P. Nguyen, Aaron W. Sanders

Contribution to the understanding of foam EOR processes: (*)

First to give experimental (coreflood) and simulation (STARS model) analysis of foam from surfactants dissolved in the gas phase

Objective of the paper:

Proving that oil recovery would be better if foam was injected in the gas phase (CO_2-Dissolved-surfactants injection)

Methodology used:

Coreflood experiments were conducted with different injection strategies including conventional conventional SAG, novel WAGS and novel CO_2.

For the simulation, a simple double-layer geological model was built in the CMG/STARS foam simulator to demonstrate the soundness of the novel foam concept.

Conclusion reached:

1. The coreflood result is that WAGS and conventional SAG give the same recovery. Continuous CO_2 injection with dissolved surfactant gives higher recovery without injected water.
2. This strategy required relatively lower injection pressure
3. The simulation results are qualitatively in good agreement with the experiments
4. A more mechanistic model for foam is needed taking into account the kinetics of surfactant partitioning between CO_2 phase and aqueous phase

Comments:

No comments

Appendix B: Grid refinement : Details and Methodology

Grid refinement

Model Name	*NX*	*NY*	*NZ*	*DX* (ft)	*DY* (ft)	*DZ* (ft)	Number of cells
Coarse Model	10	15	5	100	100	25 (average)	750

Table 9: Coarse grid characteristics

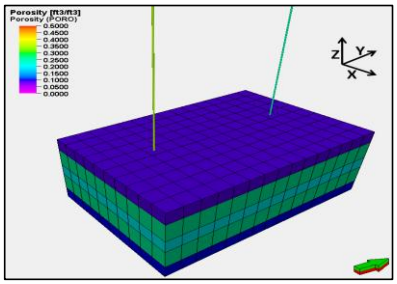

Figure 30: Porosity of the coarse model

The size of the grid has a big impact on the gas breakthrough time, and the numerical dispersion effect needs to be diminished. Starting from a coarse grid of 750 cells, with the FAWAG strategy, this part aims to increase the number of cells gradually until the number of cells has no more impact on the production results, or at least, gives a compromise between a model that will give accurate results and a model that will run reasonably fast. We start from our initial (10;15;5) cells model, and after going until a (20;60;40) intermediate model (48 000 cells) the gas breakthrough is still changing. Then we have focused on each direction individually, leaving the two other with a fixed number of divisions, to measure the influence of each direction. We have particularly observed the Gas production rate, which seems to be the most sensitive with grid size.

Sensitivity in the Z-direction

Model Name	NX	NY	NZ	DX (ft)	DY (ft)	DZ (ft)	Number of cells
ModelZ1a	80	120	20	12.5	25	6 (avg)	192 000
ModelZ1b	80	120	40	12.5	12.5	3 (avg)	384 000
ModelZ2a	20	120	40	50	12.5	3 (avg)	96 000
ModelZ2b	20	120	80	50	6.25	1.5 (avg)	192 000

Table 10: Details of the grid used to refine in the Z-direction

The number of cells in the Z-direction has the biggest influence, due to the heterogeneities of the layered reservoir, and to the impact of gravity in the WAG and FAWAG process. The process has been to compare ModelZ1a and Model Z1b to see if a model with 20 layers or 40 layers give different production profiles. Then, a comparison between ModelZ2a and Model Z2b has been done to see the difference between 40 layers and 80 layers. We can see in the plots below that the difference is important between ModelZ1a and ModelZ1b, with a breakthrough difference superior to 6 months and reasonable between modelZ2a and ModelZ2b. This leads us to choose a number of cells in the Z direction of 40.

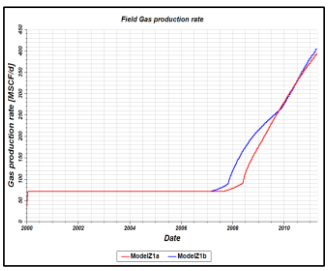

Figure 31: Gas production rate for model Z1a and Model Z1b

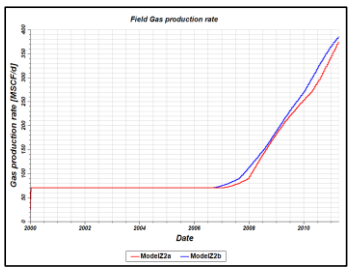

Figure 32: Gas production rate for Model Z2a and model Z2b

Sensitivity in the Y-direction

Starting from our grid (20;60;40), we increase the number of cells in the Y direction. We have tested the model described in the table below, with NY going from 60 to 240.

Model Name	NX	NY	NZ	DX (ft)	DY (ft)	DZ (ft)	Number of cells
ModelY1	20	60	40	50	25	3 (avg)	24 000
ModelY1b	20	120	40	50	12.5	3 (avg)	48 000
ModelY2	40	120	40	25	12.5	3 (avg)	192 000
ModelY2b	40	240	40	25	6.25	3 (avg)	384 000

Table 11: Details of the grid used to refine in the Y-direction

A comparison between ModelY1 and ModelY1b has been done, and another between ModelY2 and ModelY2b. The impact on the number of cells is less notable in the second case, with the comparison between ModelY2 and ModelY2b. The choice of number of cells in the Y-direction will also be 120.

Sensitivity in the X-direction

As the producers and injectors are in the Y direction, the flow is mono-directional and the X direction refining has a small influence. The number of columns in this direction is 40.

Numerical dispersion

The effect of the numerical dispersion is notable, as seen in *fig.33*. Numerically, if we consider that the breakthrough occur when the gas production rate is 1% higher than the gas production plateau rate. In the coarse grid, the breakthrough time occurs after 2715 days and 2714 days respectively, and for the fine grid, it occurs after 2139 days and 2204 days respectively.

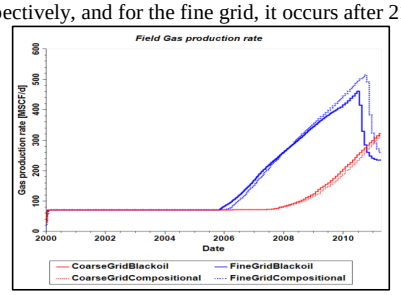

Figure 33: Effect of numerical dispersion: difference of gas production rate between the coarse grid and the fine grid

Fine Grid

Finally, our model will have the same reservoir characteristics and WAG strategy as described in *table 6*, but the water contains the foam surfactant (SAG strategy) and the grid is finer.

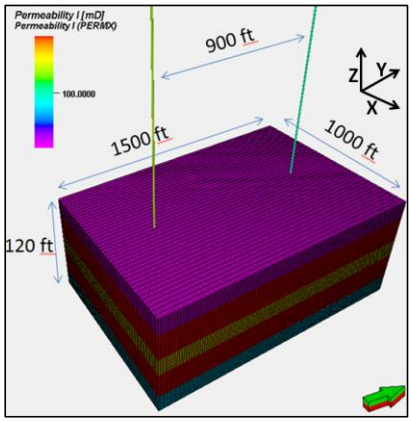

Figure 34: Permeability for the fine grid

Fine Grid & SAG strategy characteristics	
Number of cells	192 000
(NX, NY, NZ)	(40, 120, 40)
(DX, DY, DZ) (avg, in feet)	(25, 12.5, 3)
C_s^r	0.023 lbm/stb
C_s	0.6 lbm/stb

Table 12: Final Grid & FAWAG strategy characteristics

Appendix C: Influence of the mass and volume of the chemical surfactant

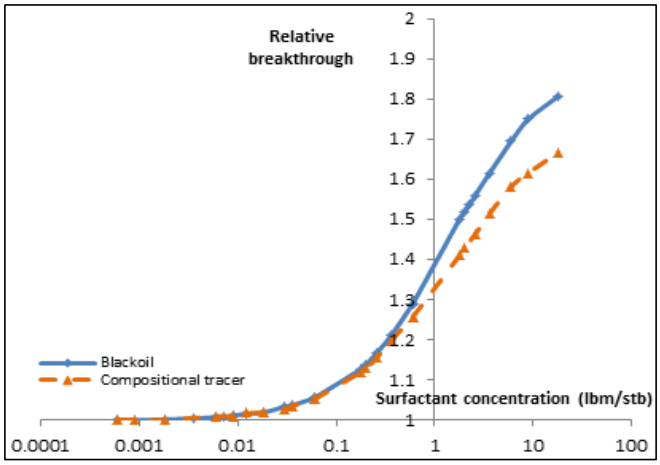

Figure 35: Relative breakthrough time as a function of the surfactant concentration. In this case, the surfactant of the compositional case has the same viscosity and molar weight .

One possible explanation for the difference between both simulators when injecting high concentration of surfactant could come from the physical presence of the foam in the compositional case. Indeed, one major difference between both simulators is that in one case the foam is a tracer, in the other case it is a chemical reactant, with a mass, and a volume. In the *fig. 35*, we create compositional foam acting as a tracer like in the blackoil simulator. The molar mass and viscosity of the foam are the same as the water (18.015 kg/mol and 0.31 cp), this way, the foam seems "invisible" to the water.

As we can see, this process improve a lot the shape of the compositional case, which is the same as the blackoil case. However, at high $\frac{C_s}{C_s^r}$ the blackoil still has a more effective foam, because the breakthrough is higher for the same concentration.

Appendix C: Visual comparison

Base Case(0.6 lbm/stb)

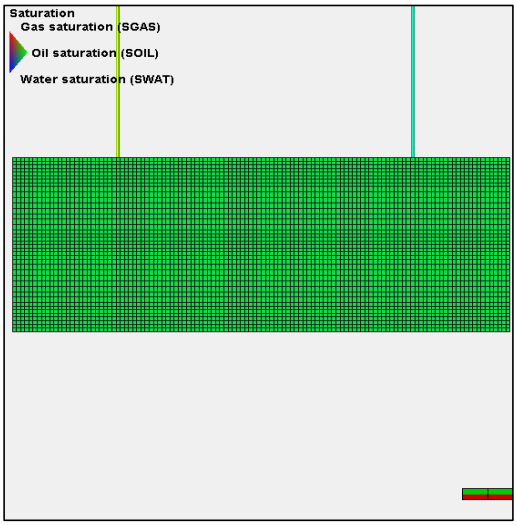

Figure 36: Blackoil - January 2000

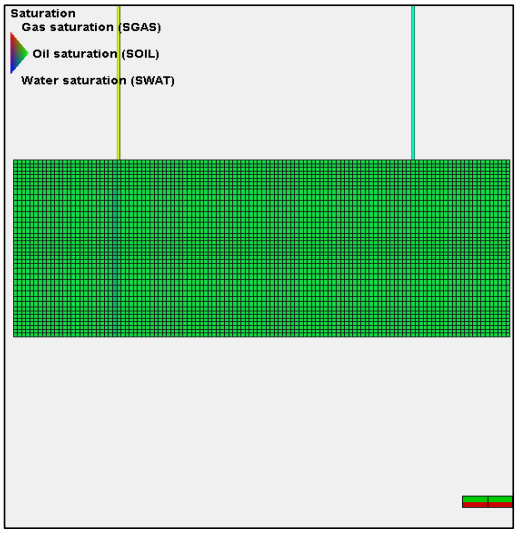

Figure 37: Compositional - January 2000

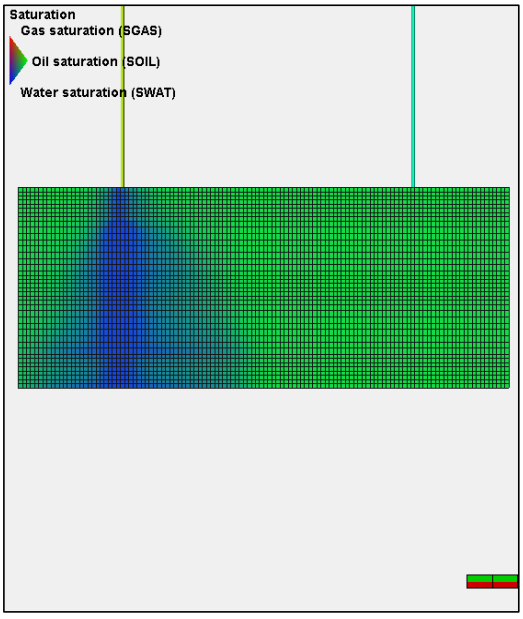

Figure 38: Blackoil - January 2002

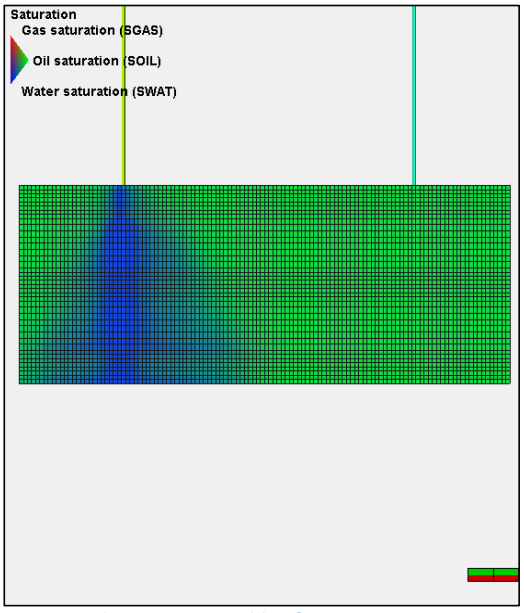

Figure 39: Compositional - January 2002

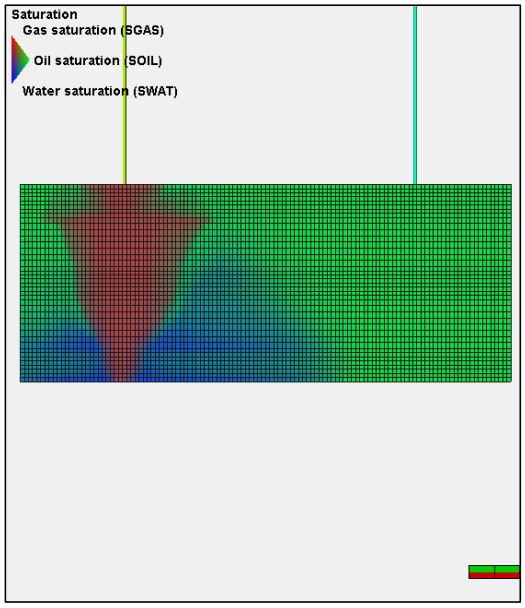

Figure 40: Blackoil - January 2004

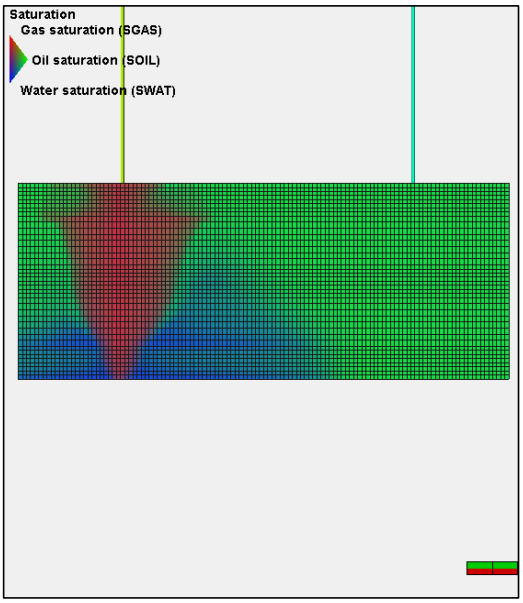

Figure 41: Compositional - January 2004

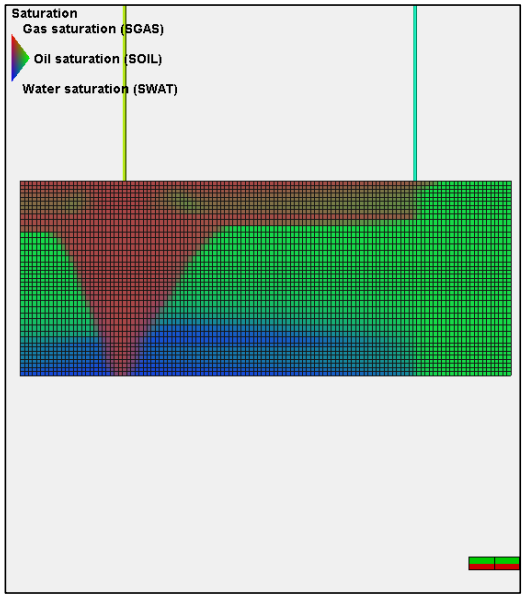

Figure 42: Blackoil - January 2007

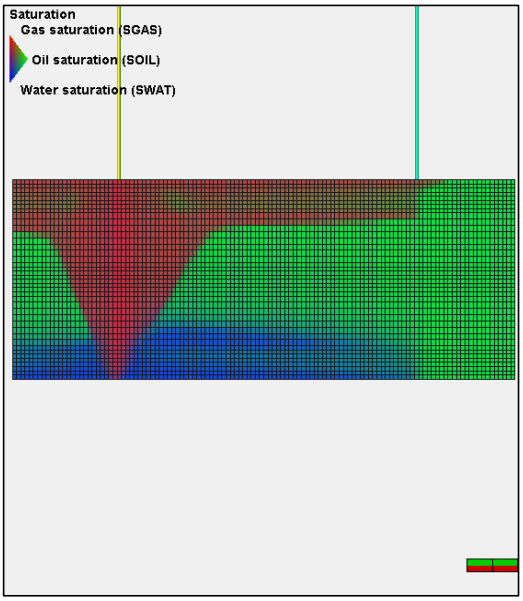

Figure 43: Compositional - January 2007

No foam

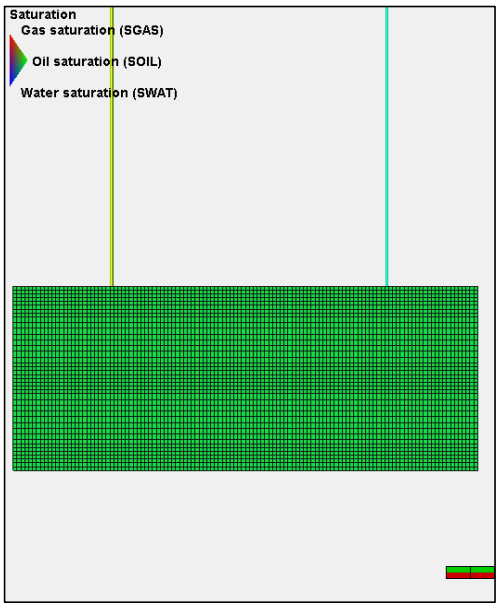

Figure 44: Blackoil - January 2000

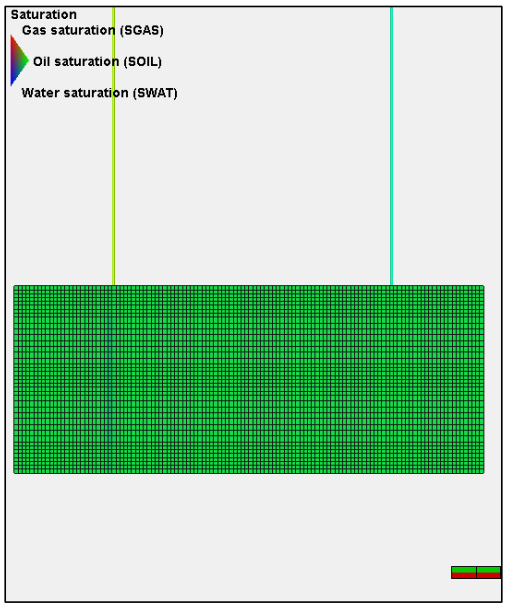

Figure 45: Compositional - January 2000

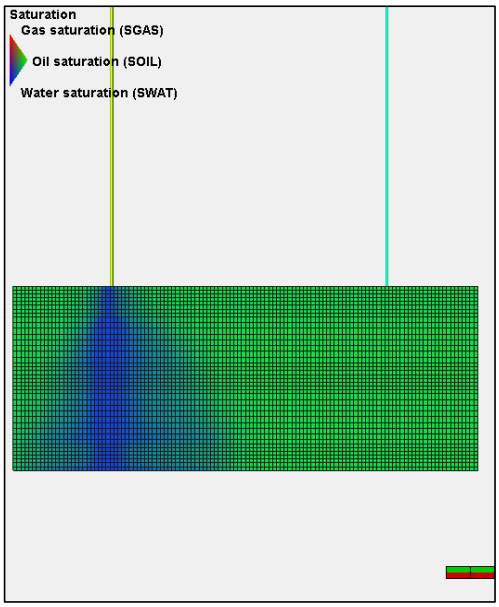

Figure 46: Blackoil - January 2002

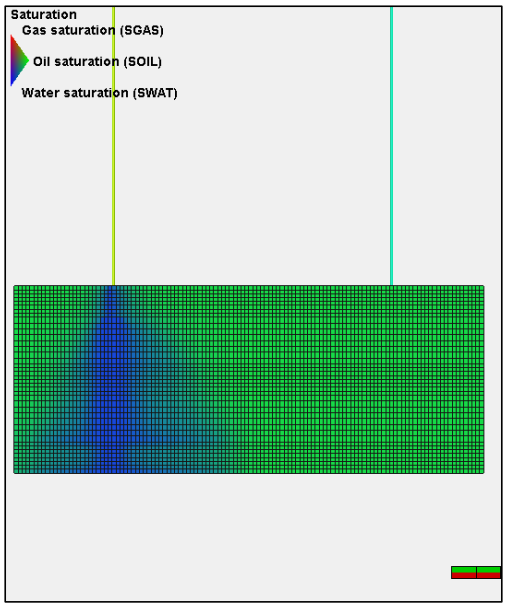

Figure 47: Compositional - January 2002

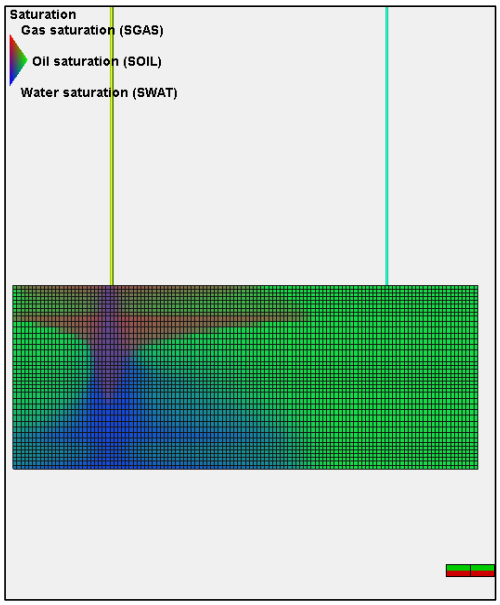

Figure 48: Blackoil - January 2004

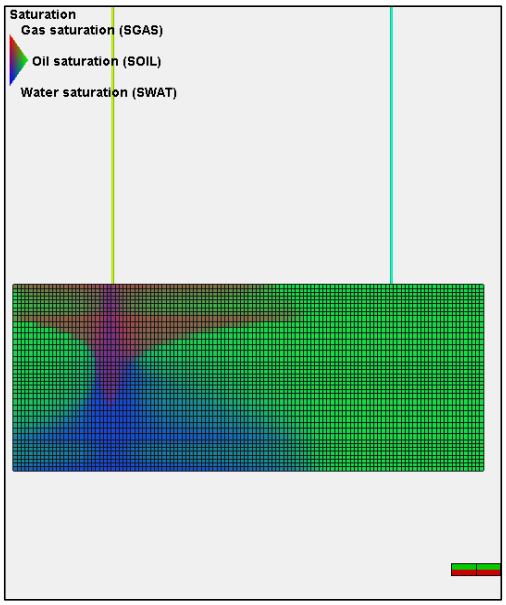

Figure 49: Compositional - January 2004

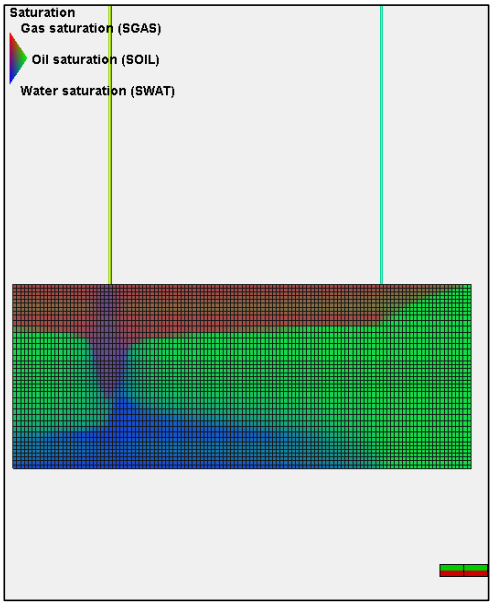

Figure 50: Blackoil - January 2007

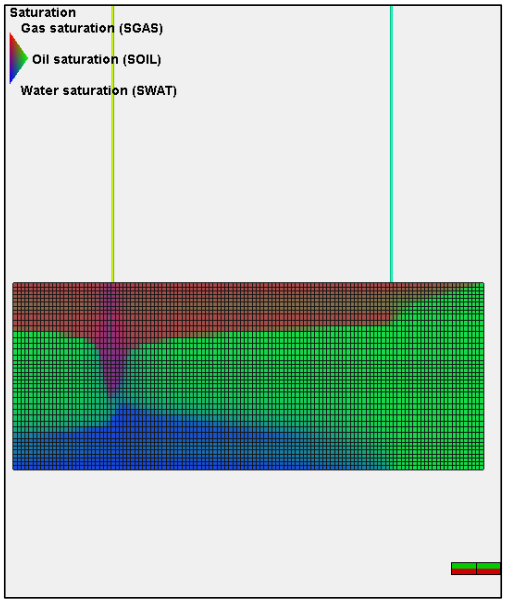

Figure 51: Compositional - January 2007

Surfactant concentration : 3lbm/stb

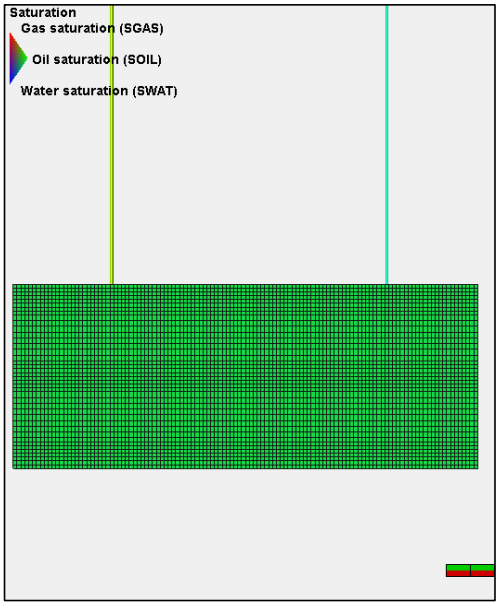

Figure 52:Blackoil - January 2000

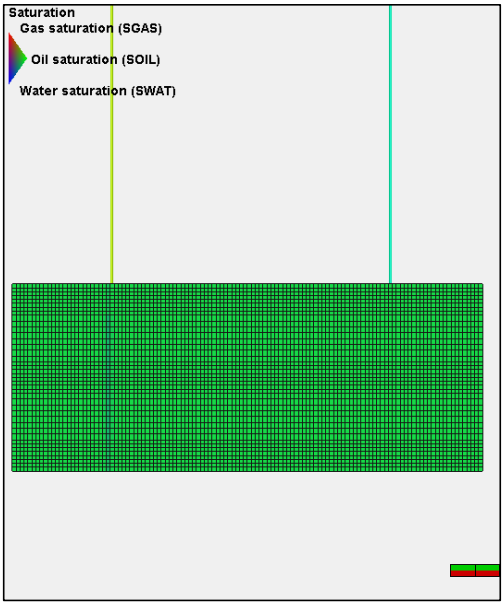

Figure 53: Compositional - January 2000

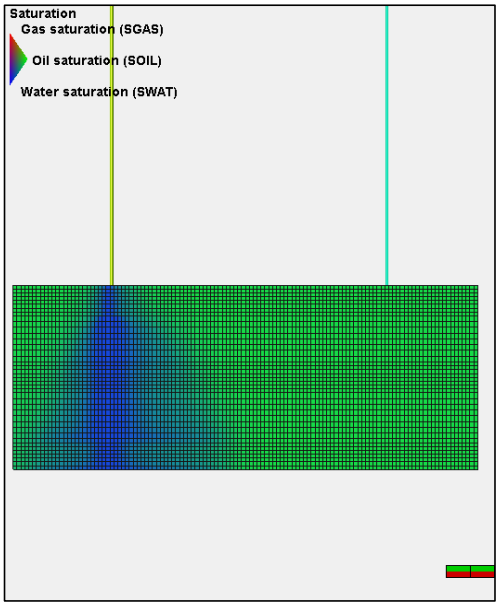

Figure 54: Blackoil - January 2002

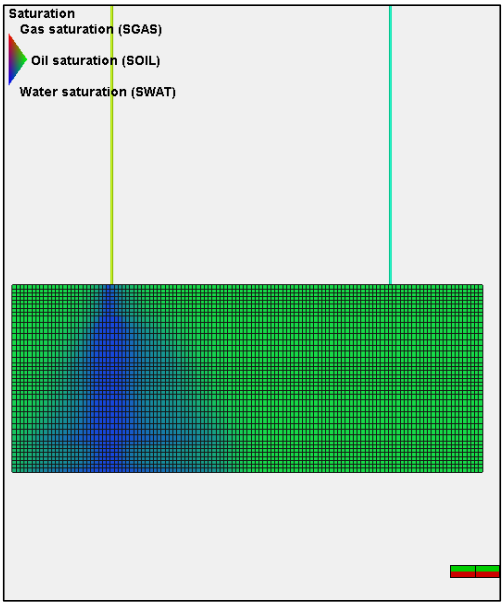

Figure 55: Compositional - January 2002

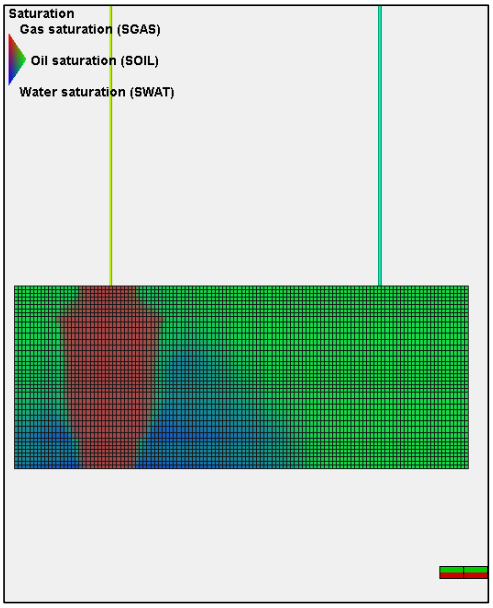

Figure 56: Blackoil - January 2004

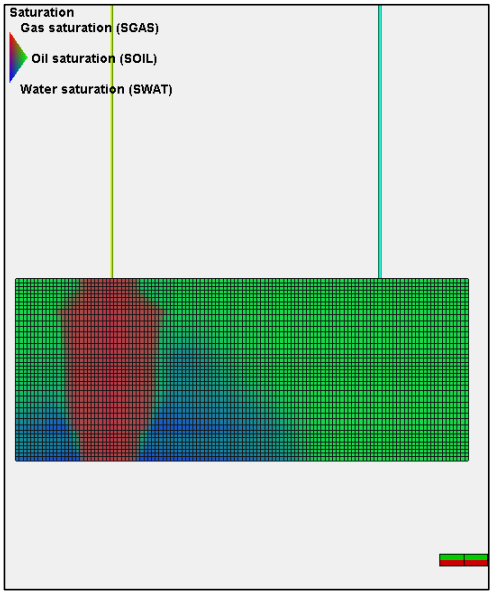

Figure 57: Compositional - January 2004

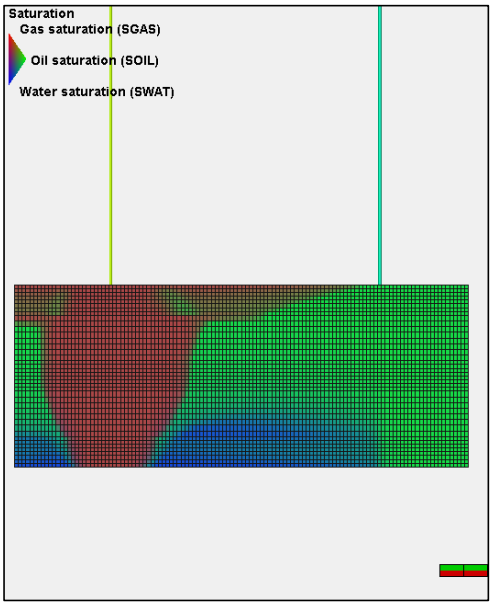

Figure 58: Blackoil - January 2007

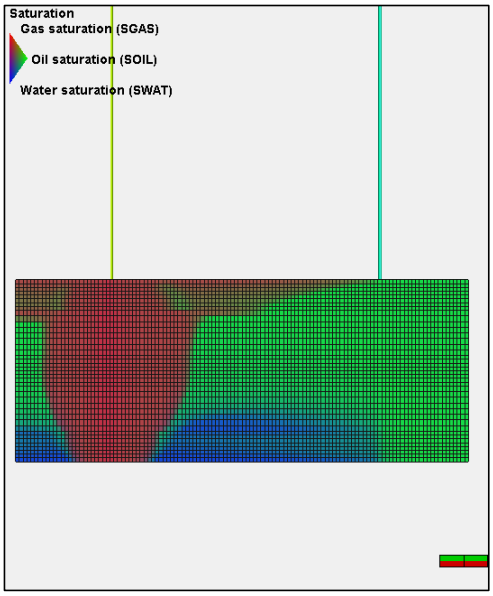

Figure 59: Compositional - January 2007

Appendix D: Eclipse *props* part for blackoil and compositional base case

ECLIPSE100 (Blackoil)

```
FOAMOPTS
WATER FUNC /



FOAMFSC
0.03  /


RPTPROPS
 'FOAM'   'DENSITY' /




ECHO
-- DENSITY created by PVTi
-- Units: lb /ft^3     lb /ft^3     lb /ft^3
DENSITY
--
-- Fluid Densities at Surface Conditions
--
       52.0719     62.4280      0.0814
/

--       'Oil GOR'    'PSAT'    'Oil FVF'    'Oil Visc'
-- Units: Mscf /stb     psia     rb /stb     cp
PVTO
--
-- Live Oil PVT Properties (Dissolved Gas)------SOME PART HAVE BEEN REMOVED FOR THE REPORT
--
        0.0000     14.6959      1.0467      2.0559
                  82.4828      1.0462      2.0677
                 150.9655      1.0458      2.0796
                 219.4483      1.0453      2.0915
                 287.9310      1.0448      2.1033
                 356.4138      1.0444      2.1150
                 424.8966      1.0439      2.1267
                 493.3793      1.0435      2.1383
                 561.8621      1.0430      2.1499
                 630.3448      1.0426      2.1614
                 698.8276      1.0421      2.1728
                 767.3103      1.0417      2.1842
                 835.7931      1.0413      2.1956
                 904.2759      1.0409      2.2069
                 966.7809      1.0405      2.2172
                1041.2414      1.0400      2.2293
                1109.7241      1.0396      2.2405
                1178.2069      1.0392      2.2516
                1246.6897      1.0388      2.2626
                1315.1724      1.0384      2.2736
                1383.6552      1.0380      2.2846
                1452.1379      1.0376      2.2955
                1520.6207      1.0373      2.3063
```

```
            1589.1034     1.0369     2.3171
            1657.5862     1.0365     2.3279
            1726.0690     1.0361     2.3386
            1794.5517     1.0358     2.3492
            1863.0345     1.0354     2.3599
            1931.5172     1.0350     2.3704
            2000.0000     1.0347     2.3809
            2032.6628     1.0345     2.3859 /
      0.4365  1657.5862     1.2929     0.5251
            1726.0690     1.2912     0.5314
            1794.5517     1.2895     0.5376
            1863.0345     1.2878     0.5439
            1931.5172     1.2862     0.5501
            2000.0000     1.2846     0.5564
            2032.6628     1.2838     0.5594 /
      0.4543  1726.0690     1.3017     0.5138
            1794.5517     1.2999     0.5199
            1863.0345     1.2982     0.5260
            1931.5172     1.2965     0.5321
            2000.0000     1.2949     0.5383
            2032.6628     1.2941     0.5412 /
      0.4722  1794.5517     1.3104     0.5028
            1863.0345     1.3087     0.5088
            1931.5172     1.3069     0.5148
            2000.0000     1.3052     0.5208
            2032.6628     1.3044     0.5236 /
      0.4902  1863.0345     1.3192     0.4922
            1931.5172     1.3174     0.4980
            2000.0000     1.3157     0.5039
            2032.6628     1.3149     0.5067 /
      0.5084  1931.5172     1.3281     0.4819
            2000.0000     1.3262     0.4876
            2032.6628     1.3254     0.4903 /
      0.5267  2000.0000     1.3369     0.4719
            2032.6628     1.3360     0.4745 /
/

-- Column Properties are:
--    'Pressure'   'Gas FVF'   'Gas Visc'
-- Units: psia     rb /Mscf     cp
PVDG
--
-- Dry Gas PVT Properties (No Vapourised Oil)
--
       14.6959    221.2339     0.0099
       82.4828     38.4265     0.0112
      150.9655     20.8498     0.0120
      219.4483     14.2666     0.0124
      287.9310     10.8196     0.0127
      356.4138      8.6992     0.0129
      424.8966      7.2638     0.0131
      493.3793      6.2282     0.0133
      561.8621      5.4463     0.0135
      630.3448      4.8354     0.0136
      698.8276      4.3452     0.0138
      767.3103      3.9434     0.0140
      835.7931      3.6083     0.0141
      904.2759      3.3247     0.0143
      966.7809      3.1016     0.0144
     1041.2414      2.8714     0.0146
```

```
      1109.7241     2.6876     0.0148
      1178.2069     2.5257     0.0149
      1246.6897     2.3821     0.0151
      1315.1724     2.2540     0.0153
      1383.6552     2.1390     0.0155
      1452.1379     2.0353     0.0157
      1520.6207     1.9413     0.0159
      1589.1034     1.8558     0.0161
      1657.5862     1.7778     0.0163
      1726.0690     1.7062     0.0165
      1794.5517     1.6405     0.0167
      1863.0345     1.5799     0.0169
      1931.5172     1.5239     0.0171
      2000.0000     1.4721     0.0173
      2032.6628     1.4486     0.0175
/


ECHO
-- Units: psia     rb /stb     /psi     cp     /psi
-- PVTW created by PVTi
PVTW
--
-- Water PVT Properties
--
       970 1.03112039169524 3.21920664108522e-006 0.312553311444583 2.56698250411855e-006
/

RPTPROPS
'SGFN'   'SWFN'   'SOF3'

/



-- WATER RELATIVE PERMEABILITY AND CAPILLARY PRESSURE ARE TABULATED AS
-- A FUNCTION OF WATER SATURATION.
--
--  SWAT   KRW   PCOW
SWFN
-- Imbibition curve
--Sw  Krw   Pc
0.2   0     6
0.25  0.01  2.6
0.3   0.025 1.6
0.35  0.04  1.1
0.4   0.065 0.7
0.45  0.09  0.5
0.5   0.125 0.36
0.55  0.16  0.2
0.6   0.2   0.12
0.7   0.275 0.04
0.8   0.35  0
1.0   0.5   0
/


SGFN
--Drainage curve
```

```
--Sg   Krg    Pcog
0      0       0.
0.02   0       0.
0.10   0.005   0.
0.15   0.015   0.
0.20   0.025   0.
0.25   0.035   0.
0.30   0.05    0.
0.35   0.065   0.
0.40   0.085   0.
0.45   0.115   0.
0.50   0.15    0.
0.55   0.19    0.
0.60   0.23    0.
0.7    0.335   0.
0.8    0.45    0.
/


SOF3
--So   Krow   Krog
0.0   0       0
0.1   0       0
0.2   0       0
0.25  0.005    0.005
0.30  0.01     0.01
0.35  0.015    0.015
0.40  0.02     0.025
0.45  0.025    0.04
0.50  0.035    0.07
0.55  0.055    0.1125
0.60  0.09     0.165
0.65  0.15     0.217
0.70  0.225    0.2875
0.75  0.32     0.36
0.80  0.45     0.45
/

-- ROCK COMPRESSIBILITY
--
--    REF. PRES   COMPRESSIBILITY
ROCK
        970          3.5D-6   /
```

ECLIPSE300 (Compositional)

```
ECHO
-- Units: psia     rb /stb     /psi     cp     /psi
-- PVTW created by PVTi
PVTW
--
-- Water PVT Properties
--
        970 1.03112039169524 3.21920664108522e-006 0.312553311444583 2.56698250411855e-006
/

-- Units: F
RTEMP
--
-- Constant Reservoir Temperature
--
        194
/

EOS
--
-- Equation of State (Reservoir EoS)
--
   PR3
/

NCOMPS
--
-- Number of Components
--
      14
/
PRCORR
--
-- Modified Peng-Robinson EoS
--
CNAMES
--
-- Component Names
--
   'CO2'
   'N2'
   'C1'
   'C2'
   'C3'
   'C4'
   'C5'
   'C6+'
   'C9+'
   'C21+'
   'C15+'
   'C29+'
   'C36+'
'Solid'
/
MW
--
-- Molecular Weights (Reservoir EoS)
```

```
--
      44.01
     28.013
     16.043
      30.07
     44.097
     58.124
     72.151
      114.2
      170.3
     352.68
      422.8
     464.89
     563.08
/

OMEGAA
--
-- EoS Omega-a Coefficient (Reservoir EoS)
--
  0.457235529
  0.457235529
  0.457235529
  0.457235529
  0.457235529
  0.457235529
  0.457235529
  0.457235529
  0.457235529
  0.457235529
  0.457235529
  0.457235529
  0.457235529
/

OMEGAB
--
-- EoS Omega-b Coefficient (Reservoir EoS)
--
  0.077796074
  0.077796074
  0.077796074
  0.077796074
  0.077796074
  0.077796074
  0.077796074
  0.077796074
  0.077796074
  0.077796074
  0.077796074
  0.077796074
  0.077796074
/

-- Units: R
TCRIT
--
-- Critical Temperatures (Reservoir EoS)
--
  548.459999999228
```

```
   227.160000017685
   343.079999988516
   549.774000004037
   665.640000033438
   755.100000003319
   838.620000015843
   1045.08380998527
   1214.77995668068
   1558.03410827381
   1652.26373977004
   1704.22006414641
   1811.53483498928
/

-- Units: psia
PCRIT
--
-- Critical Pressures (Reservoir EoS)
--
   1071.33110996644
   492.312649984577
   667.78169597908
   708.342379977809
   615.75820998071
   543.454381982975
   487.169084984738
   413.790172087037
   301.952245590541
   137.773770095684
   106.572623596661
   92.1202815071141
   66.1528539379276
/

-- Units: ft3 /lb-mole
VCRIT
--
-- Critical Volumes (Reservoir EoS)
--
   1.50573518513559
   1.44166134747024
   1.56980902280093
   2.37073199361773
   3.20369188326721
   4.1327625294147
   4.96572241906417
   7.24025487218712
   10.7417960886016
   22.4028043537099
   26.9791837569606
   29.7327196466301
   36.2354363196909
/

ZCRIT
--
-- Critical Z-Factors (Reservoir EoS)
--
   0.274077797373613
   0.291151404367252
```

```
  0.284729476638113
  0.284634795098265
  0.276164620027245
  0.277169587413721
  0.268808776311009
  0.267134146691863
  0.248807833442927
  0.184602877986906
  0.162159199184678
  0.149765133426548
  0.123305341393991
/

SSHIFT
--
-- EoS Volume Shift (Reservoir EoS)
--
  -0.04273033674
  -0.1313342386
  -0.1442656189
  -0.103268354
  -0.07750138148
  -0.05681117304
  -0.03492361458
  -0.01457986751
  0.08157562274
  0.3639855059
  0.4526016902
  0.5002401757
  0.5984269684
/

ACF
--
-- Acentric Factors (Reservoir EoS)
--
       0.225
        0.04
       0.013
      0.0986
      0.1524
      0.1956
      0.2413
  0.365930898
  0.5528269741
  1.113634874
  1.285036828
  1.377467686
  1.570808985
/

BIC
--
-- Binary Interaction Coefficients (Reservoir EoS)
--
 -0.012
    0.1   0.1
    0.1   0.1    0
    0.1   0.1    0    0
    0.1   0.1    0    0    0
```

```
    0.1    0.1      0      0      0      0
    0.1    0.1 0.037668   0.01   0.01     0     0
    0.1    0.1 0.045023   0.01   0.01     0     0     0
    0.1    0.1 0.0562072   0.01   0.01     0     0     0     0
    0.1    0.1 0.058552   0.01   0.01     0     0     0     0
      0
    0.1    0.1 0.0598178   0.01   0.01     0     0     0     0
      0     0
    0.1    0.1 0.0620616   0.01   0.01     0     0     0     0
      0     0     0
/

PARACHOR
--
-- Component Parachors
--
         78
         41
         77
        108
      150.3
      187.2
      228.9
      349.76
   453.74332
  896.6111756
  1069.574076
  1173.396216
  1415.598544
/

-- Units: ft3 /lb-mole
VCRITVIS
--
-- Critical Volumes for Viscosity Calc (Reservoir EoS)
--
  1.50573518513559
  1.44166134747024
  1.56980902280093
  2.37073199361773
  3.20369188326721
  4.1327625294147
  4.96572241906417
  7.24025487218712
  10.7417960886016
  22.4028043537099
  26.9791837569606
  29.7327196466301
  36.2354363196909
/

ZCRITVIS
--
-- Critical Z-Factors for Viscosity Calculation (Reservoir EoS)
--
  0.274077797373613
  0.291151404367252
  0.284729476638113
  0.284634795098265
  0.276164620027245
```

```
  0.277169587413721
  0.268808776311009
  0.267134146691863
  0.248807833442927
  0.184602877986906
  0.162159199184678
  0.149765133426548
  0.123305341393991
/

LBCCOEF
--
-- Lorentz-Bray-Clark Viscosity Correlation Coefficients
--
   0.1023 0.023364 0.058533 -0.040758 0.0093324
/
ZI
--
-- Overall Composition
--
       0.015
       0.008
       0.186
       0.029
        0.07
       0.078
        0.06
       0.181
       0.161
        0.06
       0.089
       0.031
       0.032
0
/

FOAMFSC
0.03  /

RPTPROPS
 'FOAM'   'DENSITY' 'SGFN'   'SWFN' /



-- ROCK COMPRESSIBILITY
--
--    REF. PRES   COMPRESSIBILITY
ROCK
      970         4.0D-6   /

--WATER PROPERTIES-----------------------------------------------------------

WNAMES
WATER FOAM SURF /

CWTYPE
 1* SURFF SURFS /

-- notice that  foam and surfactant props different from water ones
MWW
```

```
 --18.015 200 200 / Surfactant properties=/water propeties (no longer acts as a tracer)
18.015  200 200
 /

PREFW
970  5102    5102
/
--  5102 5102 5102 /

DREFW
62.428    62.4    62.4
/
--  62.4 62.4  62.4/

CREFW
3.21920664108522e-006      3.21920664108522e-006      3.21920664108522e-006
/
-- 0.0689E-10 0.0689E-10 0.0689E-10 /

VREFW
0.312553311444583   30   30
2.56698250411855e-006      2.56698250411855e-006          2.56698250411855e-006
/

-- / NOTE: surfactant has much bigger viscosity

WMFVD
 9100  1.0 0.0 0.0
 9400  1.0  0.0  0.0  /


--SURFACTANT MODEL-----------------------------------------------

-- Water/Oil surface tension vs Surfactant concentration
SURFST
-- Surfactant Water-Oil Surface Tension
-- concentration
-- lbm/ftcub lbf/ft
0.0      0.000285
0.003    0.000285
0.03121  0.000285
0.0624   0.000285
0.624    0.000285 /


-- Capillary de-saturation curve
SURFCAPD
-- LOG10(Capillary Number) Miscibility
-- Function
-9   0.0
-4.5 0.0
-2   0.0
10   0.0 /
-- /
--/
-- /

SOLWTAB
0     0.0
1.e-5 0.0
```

```
1.e-4 0.0
1.e-3 0.0
1.e-2 0.0
1.e-1 0.0 /
--/
--/
--/


--FOAM DECAY AND SURFACTANT ADSORPTION

--STOREAC
--  OIL GAS SOLS WAT FOAM SURF
--    0.0 0.0 0.0  0.0 1.0  0.0  / Decay             FOAM  -> SURF
--    0.0 0.0 0.0  0.0 0.0  1.0  / Adsoption         SURF  -> SOLID

--STOPROD
--  OIL GAS SOLS WAT FOAM SURF
--    0.0 0.0  0.0 0.0  0.0  1.0  / Decay            FOAM  -> SURF
--    0.0 0.0  1.0 0.0  0.0  0.0  / Adsoption        SURF  -> SOLID

--REACRATE
--  0.00231           -- Decay       half life = 300 days
--  0.01              -- Adsorp
-- /

--REACCORD
--  OIL GAS SOLS WAT FOAM SURF
--    0.0 0.0 0.0  0.0 1.0  0.0 /   Decay      proportional to FOAM concentration
--    0.0 0.0 0.0  0.0 0.0  1.0 / - Adsorp           proportional to SURF concentration









-- WATER RELATIVE PERMEABILITY AND CAPILLARY PRESSURE ARE TABULATED AS
-- A FUNCTION OF WATER SATURATION.
--
-- SWAT   KRW   PCOW
SWFN
-- Imbibition curve
--Sw  Krw   Pc
0.2   0     6
0.25  0.01  2.6
0.3   0.025 1.6
0.35  0.04  1.1
0.4   0.065 0.7
0.45  0.09  0.5
0.5   0.125 0.36
0.55  0.16  0.2
0.6   0.2   0.12
0.7   0.275 0.04
0.8   0.35  0
1.0   0.5   0
/
```

```
SGFN
--Drainage curve
--Sg   Krg    Pcog
0      0       0.
0.02   0       0.
0.10   0.005   0.
0.15   0.015   0.
0.20   0.025   0.
0.25   0.035   0.
0.30   0.05    0.
0.35   0.065   0.
0.40   0.085   0.
0.45   0.115   0.
0.50   0.15    0.
0.55   0.19    0.
0.60   0.23    0.
0.7    0.335   0.
0.8    0.45    0.
/


SOF3
--So   Krow   Krog
0.0   0       0
0.1   0       0
0.2   0       0
0.25  0.005    0.005
0.30  0.01     0.01
0.35  0.015    0.015
0.40  0.02     0.025
0.45  0.025    0.04
0.50  0.035    0.07
0.55  0.055    0.1125
0.60  0.09     0.165
0.65  0.15     0.217
0.70  0.225    0.2875
0.75  0.32     0.36
0.80  0.45     0.45
/




--SOLID PROPERTIES----------------------------------------------------

--CNAMES
--OIL GAS SOLID /


-- CNAMES
-- -- PROPS
-- -- Component Names
-- --
--    'CO2'
--    'N2'
--    'C1'
```

```
--    'C2'
--    'C3'
--    'C4'
--    'C5'
--    'C6+'
--    'C9+'
--    'C21+'
--    'C15+'
--    'C29+'
--    'C36+'
-- 'Solid'
-- /


CVTYPE
 13* SOLID /

MWS
13* 200  /  Same as surfactant component MWW

SDREF
 13* 62.428 /  Same as surfactant component DREFW

SCREF
 13* 3.213240147351l7e-006 /  Same as surfactant component CREFW



REGIONS

NOECHO
SATNUM
192000*1 /
--ROCKNUM
--150*1 /
EQLNUM
192000*1 /
ECHO
```